

1 We greatly appreciate the thorough review and helpful comments and suggestions.  
2 Our point-by-point responses are as follows.

3  
4 **[Reviewer 1]**

5 **General comments**

6 First, the manuscript should undergo extensive language editing. Although I am not a  
7 native speaker of English, I can notice that a lot of sentences in this manuscript,  
8 mostly in the Introduction section, are composed of too many clauses and are often  
9 hard to understand. Second, section ‘4 Historical changes’ can be improved, in both  
10 contents and structure (see below for detail). Third, the use of CMIP6 data in  
11 comparing with FireMIP model simulations sounds like a bit of circular argument to  
12 me, since results from 6 FireMIP models were used in the creation of CMIP6  
13 reconstruction. I believe this paper will be an important contribution to the fire  
14 community once these issues are adequately addressed.

15  
16 **Reply:** (1) The language has been edited extensively to improve the readability.

17  
18 (2) Contents and structure in Sec. 4 have been revised. Please see response to  
19 your specific comments below for details.

20  
21 (3) This study provides and analyzes simulation data from each of nine  
22 FireMIP models. Fire history in CMIP6 data is estimated using fire proxy  
23 data (charcoal records and visibility records) for North America, Europe,  
24 Equatorial Asia, and central Amazon, and only the median of the  
25 simulations from six FireMIP models in each grid cell for other regions.  
26 Fire proxy data are independent of FireMIP model simulations.  
27 Multi-model medians/means are sometimes used as benchmarks to  
28 compare with simulations of single models in Earth system research (e.g.,  
29 Lawrence et al. 2007, Journal of Hydrometeorology), so we think it is  
30 appropriate to compare them although they are not entirely independent.  
31 For clarification, we have changed “FireMIP models” to “median of six  
32 FireMIP model simulations” when describing the sources of CMIP6 fire  
33 emissions in Table 5 (Table 4 in the old version).

34  
35  
36 **Specific comments**

37 1. Complex or ambiguous sentences in the ‘Introduction’ (an incomplete list):

38 1) L66-69: This sentence seems too complex. The four ‘and’ and one ‘as well as’  
39 used in this single sentence make it hard to be understood.

40 **Reply:** The sentence has been rephrased as “Our study provides an important dataset  
41 for further development of regional and global multi-source merged historical  
42 reconstructions, analyses of the historical changes in fire emissions and their  
43 uncertainties, and quantification of the role of fire emissions in the Earth  
44 system.”

45  
46  
47  
48  
49  
50  
51  
52  
53  
54  
55  
56  
57  
58  
59  
60  
61  
62  
63  
64  
65  
66  
67  
68  
69  
70  
71  
72  
73  
74  
75  
76  
77  
78  
79  
80  
81  
82  
83  
84  
85  
86  
87

2) L81-89: Similarly, this sentence is way too long. The last clause (regarding the ‘air quality’) should belong to a separate sentence.

**Reply:** According to your suggestion, we have divided the sentence into three as “Second, by changing the atmospheric composition, fire emissions affect the global and regional radiation balance and climate (Ward et al., 2012; Tosca et al. 2013; Jiang et al., 2016; Grandey et al., 2016; McKendry et al., 2019; Hamilton et al., 2018; Thornhill et al., 2018). Third, fire emissions change the terrestrial nutrient and carbon cycles through altering the deposition of nutrients (e.g., nitrogen, phosphorus), surface ozone concentration, and meteorological conditions (Mahowald et al., 2008; Chen et al., 2010; McKendry et al., 2019; Yue and Unger, 2018). In addition, they degrade the air quality (Val Martin et al., 2015; Knorr et al., 2017), which poses a significant risk to human health...”

3) L93-94: The authors are too assertive in some claims and statements, in my opinion. For instance, in both cases of ‘fire emissions are estimated based on. . .’ and ‘Satellite based fire emission estimates are derived from. . .’, it may be better to use more modest expressions such as ‘are often estimated. . .’, or ‘are primarily derived from. . .’

**Reply:** We have revised sentences that are too assertive. For instance, the two sentences you mentioned have been changed to “are often estimated...” and “are primarily derived from...” as you suggested.

4) L98-99: ‘Data are available globally, but only cover the present-day period’. What ‘Data’ are you exactly talking about, (general) fire emission data, or satellite-based fire emission data? Please be more specific.

**Reply:** “data” has been changed to “Satellite-based fire emission estimates”.

5) L100-101: ‘and CO concentration trapped in. . .’. It is the CO who gets trapped, not the ‘concentration’.

**Reply:** “records of..., and CO concentration trapped in ice cores” has been changed to “ice-core records of..., and CO”

6) L104-108: Again, I have a problem in understanding this ‘complex’ sentence, partly C2 due to the 6 ‘and’/‘or’ appearances in the final clause.

**Reply:** The sentence has been divided into two as “Fire proxies can be used to reconstruct fire emissions on a local to global scale and for time periods of decades to millennia and beyond. However, fire proxies...”

## 2. Section 4: Historical changes:

1) Sections 4.1 and 4.2 are not well separated (even their titles are similar). The drivers of historical changes are discussed at the end of 4.1 and also in 4.2. Is it better

88 to move all contents of drivers to section 4.2, and switch the section titles of 4  
89 (Historical changes) and 4.1 (Historical changes and drivers)?

90 **Reply:** We agree with the reviewer. We have moved the discussion about the content  
91 of drivers from Sec. 4.1 to Sec. 4.2, and changed the titles of Secs. 4, 4.1, and  
92 4.2 to “Historical changes and drivers”, “Historical changes”, and “Drivers”,  
93 respectively.

94  
95 2) L359-360: Any theoretical explanation on the lower amplitude of seasonality from  
96 JSBACH-SPITFIRE model?

97 **Reply:** We have added “likely caused by parameter setting in its fuel moisture  
98 functions (Table S9 in Rabin et al. (2017))”.

99  
100 3) L440-441: Can you expand the explanation a little bit? i.e., how did ‘assuming no  
101 fires over croplands and setting high fuel bulk density for pastures’ lead to the sign  
102 change in LULCC response in JSBACH model?

103 **Reply:** As suggested, we have expanded the explanation to “In JSBACH-SPITFIRE,  
104 as croplands and pastures expand over time, the assumption of no fire over  
105 croplands tends to decrease fire emissions, while the setting of high fuel bulk  
106 density for pastures tends to increase fire emissions due to increased fuel  
107 combusted per burned area, which together partly result in the shifted sign of  
108 response to LULCC around the 1940s.”.

109  
110 4) Section 4.3: I like the discussions of drivers of global changes in section 4.2. But I  
111 would also like to see how these drivers play different roles on a regional scale.

112 **Reply:** We have added 14 figures in the supplementary material (Figs. S6–19) which  
113 are similar to Fig. 7 (global) but for 14 regions, to show the role of drivers on  
114 a regional scale.

115 Also, we have added a new paragraph to briefly describe them in Sec. 4.3 as  
116 “The long-term changes of regional fire emissions and inter-model  
117 disagreement are mainly caused by simulated responses to LULCC and/or  
118 population density change for the 20th century (Figs. S6–19). Besides, climate  
119 change also plays an important role in North America, northern South  
120 America, Europe, northern Africa, boreal and central Asia, and Australia.  
121 FireMIP models generally simulate increased regional fire emissions with  
122 increased CO<sub>2</sub> concentration and negligible impacts due to changes in  
123 lightning frequency, similar to the responses of global fire emissions.”

124  
125 3. Possible circular reasoning. According to the text in L303-308, CMIP6 estimates  
126 were calculated using different data sources (including 6 FireMIP model results). But  
127 the details of the reconstruction process were not given in the manuscript. How large  
128 do the FireMIP model results contribute to global emissions in CMIP6? Regardless of  
129 the amount of this fraction, some agreements between FireMIP and CMIP6 shown in  
130 Figures 6 and 9 are likely due to the use of the same data source. If you plot similar  
131 figures using data in North America + Europe + Equatorial Asia + central Amazon

132 (where no FireMIP information is used in CMIP6) only, the comparisons will be  
133 independent and maybe more convincing.

134  
135 **Reply:** Please see the response to your general comment for the comparison between  
136 FireMIP simulations and CMIP6 estimates above.

137  
138 We have revised the Fig. 9, which now provides a comparison between  
139 CMIP6/CMIP5 and simulations of FireMIP models in boreal North America,  
140 temperate North America, Europe, Equatorial Asia, NH South America, and  
141 SH South America. A brief description about them are in the revised Paras. 2  
142 and 3 of Sec. 4.3.

143  
144 In addition, Figs. 8–11 in van Marle et al. (2017, paper for CMIP6 fire  
145 emissions) already compared simulations of FireMIP models and their median  
146 with historical fire emission reconstructions based on charcoal records and  
147 visibility data (i.e. CMIP6 estimates) in four sub-regions of North America,  
148 Europe, and Equatorial Asia, and central Amazon.

#### 151 **Other specific comments**

152  
153 **1) L330:** It will be interesting to see the combustion completeness ranges in FireMIP  
154 models other than LPJ-GUESS-GlobFIRM.

155 **Reply:** We have added combustion completeness ranges of all FireMIP models in  
156 Table 2, and have changed the sentence to “...than those used in other  
157 FireMIP models (Table 2) and the satellite-based GFED family (20–40% for  
158 stem and 40–60% for coarse woody debris) (van der Werf et al., 2017).”

159  
160 **2) L492:** ‘fire and Earth science research communities’. Is fire science not a part of  
161 the Earth science?

162 **Reply:** Fire is a part of the Earth science. “fire and” has been removed.

163  
164 **3) Figure 1:** ‘CRUNCEP atm.’ shown in this figure is not easy for readers who are  
165 not familiar with reanalysis data. This can be changed to ‘atmospheric forcing’ as  
166 being consistent with that in the main text.

167 **Reply:** “CRUNCEP atm.” has been changed to “atmospheric forcing” in Fig. 1.

168  
169 **4) Figure 3.** The pattern shown in this figure is highly dependent on the spatial  
170 distribution of BC emissions. It will be good to see a map of inter-model std  
171 normalized with mean emissions.

172 **Reply:** We plotted the inter-model std normalized by mean emissions for grid cells  
173 where mean fire BC emissions were larger than  $0.001 \text{ g BC m}^{-2} \text{ yr}^{-1}$ . High  
174 values were located in regions with small mean emissions, which were in fact  
175 not important for the global fire emissions, e.g., arid regions, central

176 rainforests. Thus, we decided to keep the inter-model std map in the  
177 manuscript.

178

179 5) Figure 7: The population density is shown in the figure as ‘control run -  
180 sensitivity run’, which may cause a lot of confusion. In fact, I had a hard time  
181 understanding the meaning of ‘increasing population density’ (in L416) and  
182 ‘rising population density’ (in L421) at first, until I realized the use of this  
183 reverse scale in Figure 7. Is there any particular reason that you did not use  
184 ‘sensitivity run - control run’ instead?

185 **Reply:** Compared with ‘response to no population density change, no climate  
186 change,...’, we think ‘response to population density change  
187 (rising/increasing population density over the 20th century), climate  
188 change,...’ is more intuitive and helps better understand the simulated fire  
189 emission change shown in Fig. 6, so we used a reverse scale/‘control run -  
190 sensitivity run’ in Fig. 7.

191 To help understand Fig. 7 and related text easier, we have briefly described  
192 the control and sensitivity runs in the caption of Fig. 7 and the 20th century  
193 change of driving forces used in FireMIP in both the caption of Fig. 7 and  
194 Sec. 4.3 .

195

#### 196 **Technical corrections:**

197 1) L59: ‘most of the models’ to ‘most models’

198 **Reply:** Done

199

200 2) L116: Is it better to change ‘are applied to global change research’ to ‘have been  
201 widely used in global change research’?

202 **Reply:** Yes, changed accordingly

203

204 3) L142: In order to make it more specific, ‘Our study’ may be replaced with ‘This  
205 study’, or ‘The present study’, or ‘The study presented in this paper’, etc.

206 **Reply:** “Our study” has been changed to “This study”

207

208 4) L144: ‘the nine DGVMs’ to ‘nine DGVMs’

209 **Reply:** Done

210

211 5) L145: ‘The dataset provides the basis for’ to ‘This dataset provides a basis for’?

212 **Reply:** Done

213

214 6) L280: Why not spell out ‘CE’ for easier reading?

215 **Reply:** We have spelled CE out as “fire carbon emissions”.

216

217 7) L325-326: ‘whereas they are 1.5-4.2. . .for satellite-based products’. To be  
218 consistent with the previous clause, the range value should be in the singular form.

219 **Reply:** Changed “they are” to “it is”.

220  
221  
222  
223  
224  
225  
226  
227  
228  
229  
230  
231  
232  
233  
234  
235  
236  
237  
238  
239  
240  
241  
242  
243  
244  
245  
246  
247  
248  
249  
250  
251  
252  
253  
254  
255  
256  
257  
258  
259  
260  
261  
262  
263

**[Reviewer 2]**

**Major comments:**

1) The Authors provide a new dataset of nine fire model estimates of carbon and 33 other gas and aerosol emissions. They provide a present day analysis of the data and show that LULCC is the largest source of uncertainty when simulating historical fire emissions. The collection of this dataset is a useful step forward in synthesizing fire modelling and one which should be of great use to the climate and Earth system science community. The Authors are to be commended on such a large effort and the manuscript will be suitable for Atmospheric Chemistry and Physics once some improvements are made to the manuscript. While the content is of great interest I find myself agreeing with the previous reviewer that the grammar is not yet at a level suitable for final publication. Unfortunately, many parts of the manuscript (mainly in the first half) were hard to follow due to this. I therefore also propose an extensive review of the text. I have included some suggestions below, but it is not an extensive list.

**Reply:** Thanks for your suggestions. We have done an extensive review of the text and edited the language.

2) While the methodology and presentation of results is suitable for publication, the manuscript will benefit from further analysis in three ways. The manuscript's main objective is in presenting a dataset for use by the community, and these additions are all ways to make the manuscript more useful for that potential user: Extending the multi-model SD/zonal average plot in Figure 3 for other time slices across the dataset. A small discussion on which models are outliers for different regions/times would be insightful too. As the Authors do not know what regions will be of interest to the potential user in their studies I feel that Figure 9 should be for all regions, not just the three with the most variance, even if trends are small. Furthermore, as it is likely that the potential user will first want to compare to CMIP6, the GFED regions in Fig 8 should follow the CMIP6 version in van Marle (i.e., further segregate the Americas). Similar plots for other emissions species would also be useful and can be place in the SI.

**Reply:** 1) We have added Figs. S1b-c to show the multi-model SD/zonal average for two additional time slices, 1700–1850 and 1900–2000, and a discussion in Sec. 4.1 accordingly as “Spatial patterns of inter-model spread of fire emissions for 1700–1850 and 1900–2000 (Figs. S1b–c) are similar to the present-day patterns as shown in Fig. 3.”.

It may be unsuitable to compare the spatial patterns of SD/zonal average among different time periods in detail because 7 models are used for 1700–1850 and 9 models for 1900–2000 and 2003–2008. MC2 and CTEM do not provide simulations for 1700–1850 (Table 1), and generate lower (MC2) and higher (CTEM) historical global fire emissions than most FireMIP models for the 20th century, respectively (Fig. 6).

264 2) Fig. 9 has been revised and included all regions.  
265 Also, we have briefly described them, including outliers in these regions, in  
266 Sec. 4.3 as:  
267 “In other regions, the difference in long-term changes among models is  
268 smaller (Fig. 8b). Emissions of most models and CMIP5 estimates exhibit a  
269 significant decline in temperate North America (TENA) from ~1850 to ~1970,  
270 while historical changes of CMIP6 estimates are comparatively small (Fig. 9b).  
271 LPJ-GUESS-SIMFIRE-BLAZE has a more obvious long-term change than the  
272 other FireMIP models and CMIPs in boreal North America (BONA) and  
273 northern South America (NHSA) (Figs. 9a and d). MC2 and  
274 LPJ-GUESS-GlobFIRM emissions increase after ~1900 in Europe (EURO),  
275 while emissions of other models and CMIPs are overall constant (Fig. 9f). In  
276 boreal Asia (BOAS), emissions of most models and CMIP6 are relatively  
277 constant, while LPJ-GUESS-GlobFIRM and CMIP5 emissions decline from  
278 1850 to the 1950s and from 1900 to the 1970s, respectively, and then rise (Fig.  
279 9j). JULES, LPJ-GUESS-SIMFIRE-BLAZE, CLM4.5, CTEM, and CMIP6  
280 emissions significantly decline since the 1950s in Southeast Asia (SEAS),  
281 while CMIP5 emissions increase (Fig. 9l). In equatorial Asia (EQAS), CMIPs  
282 emissions increase after ~1950, which is partly reproduced by only CLM4.5 in  
283 FireMIP (Fig. 9m).”  
284  
285 3) We used the GFED regions because they represent key fire regions across the  
286 world and are the most widely used one by the community. In addition, Figs.  
287 10–11 in van Marle et al. (2017, paper for CMIP6 fire emissions) already  
288 compared each of FireMIP models and their medians with historical  
289 charcoal-based reconstructions (i.e. CMIP6 estimates) in four sub-regions of  
290 North America, so we did not want to repeat the same analyses here.  
291  
292 4) As suggested, we have added Figs. S3–5 for regional fire BC, OC, and CH<sub>4</sub>  
293 emissions in the supplementary material, and the words “As shown in Figs.  
294 S3–5, long-term changes of regional fire emissions for other species are  
295 similar to those of fire CO emissions.” in Sec. 4.3.  
296  
297  
298 3) The present-day evaluation is of a suitable level for publication as is; however,  
299 further historical evaluation can be undertaken. In particular, the contribution of crop  
300 burning and how the fire models compare against historical fire proxies (not just the  
301 CMIP5/6 reconstructions). As crop fires are only accounted for in CLM, please  
302 discuss what this means in terms of missing estimates of historical emissions across  
303 FireMIP, a figure of % contribution to total emissions over time for example would be  
304 insightful. Included should be a discussion of current knowledge of crop fires in the  
305 present day, their uncertainties in emissions back in time, and what this means for  
306 CMIP/FireMIP as LULCC has been shown to be the largest uncertainty here. This  
307 then links to an overall evaluation of historical emissions with proxies. The inclusion

308 of an updated Figure similar to the one from van der Werf's 2013 paper for example?  
309 I leave it to the Authors to decide on how best to do this, but it should be included to  
310 once again help guide the potential user; perhaps in section 4.3.

311  
312 **Reply:** 1) We have compared the historical changes of the FireMIP simulations with  
313 other widely used reconstructions in global-scale fire studies and added "...,  
314 but in disagreement with earlier reconstructions based on charcoal records  
315 (Marlon et al., 2008; Marlon et al., 2016), ice-core CO records (Wang et al.,  
316 2010), and ice-core  $\delta^{13}\text{CH}_4$  records (Ferretti et al., 2005), which exhibit a rapid  
317 increase from 1700 to roughly the 1850s."

318 and a new paragraph "Earlier reconstructions based on fire proxies also show a  
319 big difference in long-term changes after the 1850s. The reconstruction based  
320 on the Global Charcoal Database version 3 (GCDv3, Marlon et al., 2016)  
321 exhibits a decline from the late 19th century to the 1920s, and then an upward  
322 trend until ~1970, followed by a drop. The reconstructions based on the  
323 GCDv1 (Marlon et al., 2008) and ice-core CO records (Wang et al., 2010)  
324 show a sharp drop since roughly the 1850s, while a steady rise is exhibited in  
325 the reconstruction based on ice-core  $\delta^{13}\text{CH}_4$  records (Ferretti et al., 2005). The  
326 simulated historical changes of FireMIP models (Fig. 6) fall into this fairly  
327 broad range of long-term trends in these reconstructions." in Sec. 4.1.

328 We will perform a detailed regional comparison with reconstructions based on  
329 various fire proxies (including but not limited to charcoal records, and  
330 considering that recently more paleofire records are being compiled, e.g., the  
331 number of sites with charcoal records in China will be increased from 15 in  
332 GCDv3 to 113) and driver analyses in the near future in cooperation with  
333 scientists who work on fire proxies.

334  
335 2) We have added Fig. S2 to show the historical change of crop fire emissions  
336 in the CLM and % contribution to total emissions, and have added  
337 discussion in Sec. 5 as:

338 "Fire has been widely used in agricultural management during the harvesting,  
339 post-harvesting, or pre-planting periods (Korontzi et al., 2006; Magi et al.,  
340 2012). Crop fire emissions are an important source of greenhouse gases and  
341 air pollutants (Tian et al., 2016; Wu et al., 2017; Andreae, 2019). GFED4s  
342 reported that fires in croplands can contribute 5% of burned area and 6% of  
343 fire carbon emissions globally in the present day (Randerson et al., 2012; van  
344 der Werf et al., 2017). In FireMIP, only CLM4.5 simulates crop fires,  
345 whereas the other models assume no fire in croplands or treat croplands as  
346 natural grasslands. In CLM4.5, crop fires contribute 5% of the global burned  
347 area in 2001–2010, similar to GFED4s estimates. However, CLM4.5  
348 estimates a total of 260 Tg C yr<sup>-1</sup> carbon emissions (contribution rate: 13%),  
349 which is higher than the GFED4s estimate (138 Tg C yr<sup>-1</sup>) because CLM4.5  
350 simulates higher fuel loads in croplands than the CASA model used by  
351 GFED4s. In CLM4.5, both the carbon emissions from crop fires and the

352 contribution of crop fire emissions to the total fire emissions increase  
353 throughout the 20th century (Fig. S2), which is consistent with earlier  
354 estimates based on a different crop fire scheme (Ward et al., 2018). In  
355 JULES-INFERNNO, an increase in cropland area also leads to an increase in  
356 burned area and fire carbon emissions because this model treats croplands as  
357 natural grasslands. Grasses dry out faster than woody vegetation and are  
358 easier to burn, so an increasing cropland area leads to increasing burned area  
359 and fire carbon emissions. On the other hand, for FireMIP models that  
360 exclude croplands from burning, expansion of croplands leads to a decrease  
361 in burned area and fire carbon emissions. Therefore, different treatment of  
362 crop fires can contribute to the uncertainty in simulated fire emissions. Since  
363 four out of six FireMIP models used for generating CMIP6 estimates exclude  
364 croplands from burning (van Marle et al., 2017b), CMIP6 estimates may  
365 underestimate the impact of historical changes of crop fire emissions in some  
366 regions (e.g., China, Russia, India). Given the small extent of crop fires, high  
367 resolution remote sensing may help improve the detection of crop fires  
368 (Randerson et al., 2012; Zhang et al., 2018), which can benefit the driver  
369 analyses and modeling of historical crop fires and their emissions in  
370 DGVMs.”.

371  
372 **Minor comments:**

373 1) Lines 61-62. The statement ‘consistent with multi source merged historical  
374 reconstructions’ is in reference to CMIP5/6; however, a multi-source merged  
375 historical reconstruction of the proxy data (ice cores, charcoal, tree scars etc.) would  
376 not result in the same conclusion. Please either rephrase in terms of CMIP, add that  
377 this disagrees with proxies, or remove.

378 **Reply:** We have added “as input data for CMIP6”

379  
380 2) Line 77: Species emitted from fires

381 **Reply:** Done

382  
383 3) Lines 81-89: I think this sentence needs to be clearer, both in grammar and content.  
384 Are all the items in the list symptoms of the atmospheric composition changing in  
385 response to fires? For example, changes to the ‘terrestrial nutrient and carbon cycles’  
386 are more a symptom of changes to the magnitude of deposition and alteration to the  
387 land vegetation itself and the human health impacts are linked to the air quality  
388 changes (as R1 has also mentioned). Perhaps writing as a numbered list would help?

389 **Reply:** The sentence has been changed to “ Second, by changing the atmospheric  
390 composition, fire emissions affect the global and regional radiation balance  
391 and climate (Ward et al., 2012; Tosca et al. 2013; Jiang et al., 2016; Grandey  
392 et al., 2016; McKendry et al., 2019; Hamilton et al., 2018; Thornhill et al.,  
393 2018). Third, fire emissions change the terrestrial nutrient and carbon cycles  
394 through altering the deposition of nutrients (e.g., nitrogen, phosphorus),  
395 surface ozone concentration, and meteorological conditions (Mahowald et al.,

396 2008; Chen et al., 2010; McKendry et al., 2019; Yue and Unger, 2018). In  
397 addition, they degrade the air quality (Val Martin et al., 2015; Knorr et al.,  
398 2017), which poses a significant risk to human health... ”

399

400 4) Line 90: There have been observation campaigns, such as SAMMBA, which have  
401 attempted to observe aerosol from fires at the regional scale using a combination of  
402 ground based and aircraft measurements. While they are only snap shots, due to the  
403 inherent time limitations of campaigns (as compared to say satellites), for  
404 completeness I would ask the Authors to list some of these as attempts to bridge that  
405 gap.

406 **Reply:** As suggested, we have added “some attempts have been made to bridge the  
407 gap between local observations and regional estimates using combinations of  
408 aircraft and ground based measurements from field campaigns (e.g.,  
409 SAMBBA, ARCTAS), satellite-based inventories, and chemical transport and  
410 aerosol models (e.g., Fisher et al., 2010; Reddington et al., 2019; Konovalov et  
411 al., 2018).”

412

413 5) Line 99: Define ‘present day period’, i.e. list years data available.

414 **Reply:** We have added “i.e., since 1997 for GFED and shorter periods for others”.

415

416 6) Line 100: Suggest altering to say something like ‘gases such as . . .’ as they way it  
417 is currently presented appears to be a definitive list but is not. For example, vanillic  
418 acid has also been used as a unique tracer of fires. Please also make it clear that is the  
419 C3 methane carbon isotope which is the tracer, as this species has many sources.

420 **Reply:** In the revised version, we have rephrased the sentence as “Historical change  
421 of fire emissions has been inferred from a variety of proxies, such as ice-core  
422 records of CH<sub>4</sub> (isotope  $\delta^{13}\text{CH}_4$  from pyrogenic or biomass burning source),  
423 black carbon, levoglucosan, vallic acid, ammonium, and CO (Ferretti et al.,  
424 2005; McCornnell et al., 2007; Conedera et al., 2009; Wang et al., 2012;  
425 Zennaro et al., 2014), site-level sedimentary charcoal records (Marlon et al.,  
426 2008, 2016), visibility records (van Marle et al., 2017a), and fire-scar records  
427 (Falk et al. 2011).”

428

429

430 7) Line 104: Can the authors add a few words to describe aerosol indices, it is  
431 perhaps not as common as the others and would aid in reader comprehension.

432 **Reply:** The aerosol index represents the amount of absorbing aerosols. We have  
433 removed it, and changed to “fire-scar records” which is more commonly used.

434

435 8) Lines 104-109: Suggest that the Authors add something positive here about  
436 proxies for balance. While it is true that no proxy can accurately define the past, it  
437 currently reads a bit as if you are suggesting all this work is not of any worth.

438 **Reply:** We have added “Fire proxies can be used to reconstruct fire emissions on a  
439 local to global scale and for time periods of decades to millennia and beyond.”

440

441 9) Lines 117:119: Suggest: 'Fire emissions of trace gases and aerosols are derived  
442 from the product of the simulated DGVM carbon emission and a species emission  
443 factor (Li et al., 2012; Knorr et al., 2016).'

444 **Reply:**Done

445

446 10) Line 185: 'their estimates of' rather than 'the simulations of'

447 **Reply:** Done

448

449 11) Line 186: remove comma

450 **Reply:** Done

451

452 12) Line 190-195: Much of this is not grammatically correct, please rephrase.

453 **Reply:** Changed to "CLM4.5 models fires in croplands, human deforestation and  
454 degradation fires in tropical closed forests, and human ignition and  
455 suppression for both occurrence and spread of fires outside of tropical closed  
456 forests and croplands."

457

458 13) Lines 227-235: The information in this paragraph could come before the protocol  
459 in the paragraph before. Such that when reading the protocol, it is clear where the data  
460 is from already.

461 **Reply:** Reordered as suggested.

462

463 14) Line 255: See Andrea (2019) for details; as this paper is only in prep I would  
464 suggest not explicitly directing the reader to it for more details.

465 **Reply:** The manuscript was published recently. We have updated the reference.

466

467 15) Line 255-256: Suggest: 'All FireMIP model simulations used the same EFs from  
468 Table 2.'

469 **Reply:** Done

470

471 16) Line 261: Incorrect placing of semi-colon (should be a comma), it could however  
472 be placed before 'similar' if wanted. Also suggest adding 'are classified as' for each  
473 of the three PFT instances not just the first.

474 **Reply:** The sentence has been divided into two, so the semi-colon is now a period.  
475 Also, the words "are classified as" have been added.

476

477 17) Line 287: please define 'them'

478 **Reply:** "them" has been replaced by "satellite-based estimates of present-day fire  
479 emissions".

480

481 18) Line 316: The definition of discrepancy is 'a difference between two figures,  
482 results, etc. that are expected to be the same'. I do not think these results should be

483 expected to be the same as the underlying factors have uncertainties in their  
484 representations, as the Authors mention?

485 **Reply:** “discrepancy” has been changed to “difference”.

486

487 19) Line 317: Emissions are ‘from’ the land, not ‘over’ them which is the  
488 concentration. Suggest to double check for occurrences elsewhere.

489 **Reply:** all “over the land” have been changed to “from the land”

490

491 20) Lines 347-350: More details here please. . . Why? Which models are driving this  
492 variability? Do satellites suggest this is a variable region too? etc.

493 **Reply:** We have added “This is mainly driven by the MC2, CTEM,  
494 JSBACH-SPITFIRE, and ORCHIDEE-SPITFIRE simulations (Fig. 2).” and  
495 “The differences among the satellite-based estimates have a similar spatial  
496 pattern, but higher than the inter-model spread in savannas over southern  
497 Africa and lower in the temperate arid and semi-arid regions and north of  
498 60°N over Eurasia (Fig. S1a).” in Sec. 3.1.

499 Furthermore, we have added Fig. S1a in Supplementary Material which is  
500 similar to Fig. 3 but for satellite-based estimates of fire emissions.

501

502 21) Lines 402-403: But in disagreement with the ice-core/tree scar/charcoal proxies?  
503 These show variability in emissions from 1700-1900, with a peak ~1850?

504 **Reply:** Yes. We have added “but in disagreement with earlier reconstructions based  
505 on charcoal records (Marlon et al., 2008; Marlon et al., 2016), ice-core CO  
506 records (Wang et al., 2010), and ice-core  $\delta^{13}\text{CH}_4$  records (Ferretti et al.,  
507 2005), which exhibit a rapid increase from 1700 to roughly the 1850s. ”

508

509 22) Lines 531-535 and 547-550: If most models do not capture these trends does it  
510 not therefore suggests that historical emissions are likely underestimated in most fire  
511 models (and hence also CMIP6)?

512 **Reply:** Yes, it does.

513 We also note that besides human suppression on fire spread and the decrease  
514 in fuel continuity from expanding croplands and pastures (Lines 531–535 and  
515 547–550 in old version), human deforestation and degradation fires and crop  
516 fires are not modeled by most FireMIP models which can also affect the  
517 simulations of historical fire emissions. At this stage, we are unclear about the  
518 net effect of these factors. We think this is an important point to address and  
519 have added a discussion in Sec. 5 (see response to your next comment below).

520

521 23) Line 551: The conclusions appears to stop a bit abruptly, could the authors finish  
522 the conclusions on an outlook or implication etc. to tie it all together a bit more. One  
523 example, global CMIP6 emissions are basically flat w.r.t. time, and so using model  
524 emissions which are much more variable will result in a different simulated  
525 climate/Earth system response.

526 **Reply:** Thank you for this suggestion. We have added a paragraph in Conclusions as  
527 “As discussed above, most FireMIP models do not consider the human  
528 suppression of fire spread, decreased fuel continuity from expanding  
529 croplands and pastures, human deforestation and degradation fires, and crop  
530 fires. Therefore, these models, and hence the CMIP6 estimates that are mainly  
531 based on them, may have some uncertainties in estimating historical fire  
532 emissions and long-term trends. This may further affect the estimates of the  
533 radiative forcing of fire emissions and the historical response of trace gas and  
534 aerosol concentrations, temperature, precipitation, and energy, water, and  
535 biogeochemical cycles to fire emissions based on Earth/climate system  
536 models that include these fire models or are driven by such fire emissions. It  
537 may also influence future projections of climate and Earth system responses  
538 to various population density and land use scenarios.”.

539  
540 24) Figure 2: The lat/lon co-ordinates are too small to read. Remove as they are not  
541 actually necessary.

542 **Reply:** In the revised version, only lat labels at the rightmost and lon labels at the  
543 bottom are retained but with a bigger font size as some readers may want to  
544 have this information, and all other lat/lon labels have been removed.

545

546 25) Figure 7: suggest moving d and e to the a and b positions then decreasing the axis  
547 limits for the other three so the differences can be seen.

548 **Reply:** We decided to use the same y axis for Figs. 7a-e so readers can easily compare  
549 the magnitude of the simulated response of fire emissions to different drivers.  
550 The main objective of Fig. 7 is to highlight the importance of simulated  
551 responses to LULCC and population density change in the inter-model  
552 disagreement of historical fire emission changes, so the same y axis seems  
553 better.

554

555

556

557

558

559

560 **Historical (1700–2012) Global Multi-model Estimates of the Fire Emissions from**  
561 **the Fire Modeling Intercomparison Project (FireMIP)**

562 Fang Li<sup>1\*</sup>, Maria Val Martin<sup>2</sup>, ~~Stijn Hantson<sup>3,4</sup>~~, Meinrat O. Andreae<sup>5,3,4</sup>, Almut  
563 Arne<sup>5,4</sup>, ~~Stijn Hantson<sup>6,5</sup>~~, ~~Johannes W. Kaiser<sup>7,3</sup>~~, Gitta Lasslop<sup>8,6</sup>, Chao Yue<sup>9,7,10,8</sup>,  
564 Dominique Bachelet<sup>11,9</sup>, Matthew Forrest<sup>8,6</sup>, ~~Johannes W. Kaiser<sup>10,5</sup>~~, Erik Kluzek<sup>12,1</sup>,  
565 Xiaohong Liu<sup>13,2</sup>, ~~Stephane Mangeon<sup>14,15</sup>~~, Joe R. Melton<sup>16,3</sup>, Daniel S. Ward<sup>17,4</sup>, Anton  
566 Darnenov<sup>18,5</sup>, Thomas Hickler<sup>8,6,19,6</sup>, Charles Ichoku<sup>20,17</sup>, Brian I. Magi<sup>21,18</sup>, Stephen  
567 Sitch<sup>22,19</sup>, Guido R. van der Werf<sup>23,9</sup>, Christine Wiedinmyer<sup>24</sup>, ~~Sam S. Rabin<sup>5</sup>~~

568 <sup>†</sup>

569 <sup>1</sup> International Center for Climate and Environment Sciences, Institute of Atmospheric  
570 Physics, Chinese Academy of Sciences, Beijing, China

571 <sup>2</sup> Leverhulme Center for Climate Change Mitigation, Department of Animal & Plant  
572 Sciences, Sheffield University, Sheffield, UK

573 <sup>3</sup> Max Planck Institute for Chemistry, Mainz, Germany

574 <sup>4</sup> Department of Geology and Geophysics, King Saud University, Riyadh, Saudi  
575 Arabia

576 <sup>3</sup> ~~Geospatial Data Solutions Center, University of California, Irvine, CA, USA~~

577 <sup>5,4</sup> Karlsruhe Institute of Technology (KIT), Institute of Meteorology and Climate  
578 research, Atmospheric Environmental Research, Garmisch-Partenkirchen, Germany

579 <sup>6</sup> Geospatial Data Solutions Center, University of California, Irvine, CA, USA

580 <sup>7</sup> Deutscher Wetterdienst, Offenbach, Germany

581 ~~<sup>5</sup> Max Planck Institute for Chemistry, Mainz, Germany~~

582 <sup>86</sup> Senckenberg Biodiversity and Climate Research Centre (BiK-F),

583 Senckenberganlage, Germany

584 <sup>97</sup> State Key Laboratory of Soil Erosion and Dryland Farming on the Loess Plateau,

585 Northwest A&F University, Yangling, Shanxi, China

586 ~~Laboratoire des Sciences du Climat et de l'Environnement, LSCE/IPSL,~~

587 ~~CEA-CNRS-UVSQ, Université Paris-Saclay, Gif-sur-Yvette, France~~

588 <sup>108</sup> Laboratoire des Sciences du Climat et de l'Environnement, LSCE/IPSL,

589 CEA-CNRS-UVSQ, Université Paris-Saclay, Gif-sur-Yvette, France

590 ~~State Key Laboratory of Soil Erosion and Dryland Farming on the Loess Plateau,~~

591 ~~Northwest A&F University, Yangling, Shanxi, China~~

592 <sup>119</sup> Biological and Ecological Engineering, Oregon State University, Corvallis, OR,

593 USA

594 ~~<sup>10</sup> Deutscher Wetterdienst, Offenbach, Germany~~

595 <sup>121</sup> National Center for Atmospheric Research, Boulder, CO, USA

596 <sup>132</sup> Department of Atmospheric Science, University of Wyoming, Laramie, WY, USA

597 <sup>14</sup> Department of Physics, Imperial College London, London, UK

598 <sup>15</sup> Now at CSIRO, Data61, Brisbane, QLD, Australia

599 <sup>163</sup> Climate Research Division, Environment and Climate Change Canada, Victoria,

600 BC, Canada

601 <sup>174</sup> Karen Clark and Company, Boston, MA, USA

602 <sup>185</sup> Global Modeling and Assimilation Office, NASA Goddard Space Flight Center,

603 Greenbelt, MD, USA

604 <sup>196</sup> Department of Physical Geography, Goethe University, Frankfurt am Main,

605 Germany

606 <sup>2017</sup> Howard University, NW, Washington, DC, USA

607 <sup>2118</sup> Department of Geography and Earth Sciences, University of North Carolina at

608 Charlotte, Charlotte, NC, USA

609 <sup>2219</sup> College of Life and Environmental Sciences, University of Exeter, Exeter, UK

610 <sup>239</sup> Faculty of Science, Vrije Universiteit, Amsterdam, The Netherlands

611 <sup>241</sup> University of Colorado Boulder, Boulder, CO, USA

612

613 \*Correspondence to: Fang Li ([lifang@mail.iap.ac.cn](mailto:lifang@mail.iap.ac.cn))

614

615

## 616 **Abstract**

617 Fire emissions are critical for carbon and nutrient cycles, climate, and air quality.

618 Dynamic Global Vegetation Models (DGVMs) with interactive fire modeling provide

619 important estimates for long-term and large-scale changes ~~in~~ fire emissions. Here

620 we present the first multi-model estimates of global gridded historical fire emissions

621 for 1700–2012, including carbon and 33 species of trace gases and aerosols. The

622 dataset is based on simulations of nine DGVMs with different state-of-the-art global

623 fire models that participated in the Fire Modeling Intercomparison Project (FireMIP),  
624 using the same and standardized protocols and forcing data, and the most up-to-date  
625 fire emission factor table ~~based on~~~~from~~ field and laboratory studies ~~in~~~~over~~ various  
626 land cover types. We evaluate the simulations of present-day fire emissions by  
627 comparing them with satellite-based products. ~~The e~~Evaluation results show that most  
628 DGVMs simulate present-day global fire emission totals within the range of  
629 satellite-based products. ~~They, and~~ can capture the high emissions over the tropical  
630 savannas ~~and~~, low emissions over the arid and sparsely vegetated regions, and the  
631 main features of seasonality. However, most ~~of the~~ models fail to simulate the  
632 interannual variability, partly due to a lack of modeling peat fires and tropical  
633 deforestation fires. ~~Before the 1850s, Historically,~~ all models show only a weak trend  
634 in global fire emissions, ~~before 1850s, which is~~ consistent with ~~the~~ multi-source  
635 merged historical reconstructions ~~used as input data for CMIP6. On the other hand,~~  
636 ~~the trends are quite different among DGVMs for the 20th century, The long-term~~  
637 ~~trends among DGVMs are quite different for the 20<sup>th</sup> century,~~ with some models  
638 showing an increase and others a decrease in fire emissions, mainly as a result of the  
639 discrepancy in their simulated responses to human population density change and  
640 land-use and land-cover change (LULCC). Our study provides ~~an important basic~~  
641 dataset for ~~further development of~~ regional and global multi-source merged  
642 historical reconstructions ~~and merging methods,~~ and ~~analyses of~~ ~~the~~ historical  
643 changes ~~of~~ fire emissions and their uncertainties, ~~and quantification as well as of~~  
644 ~~their~~ role ~~of fire emissions~~ in the Earth system. It also highlights the importance of

645 accurately modeling the responses of fire emissions to LULCC and population density  
646 change in reducing uncertainties in historical reconstructions of fire emissions and  
647 providing more reliable future projections.

648

649

## 650 **1. Introduction**

651 Fire is an intrinsic feature of terrestrial ecosystem ecology ~~globally, and has~~  
652 emerged occurring in all major biomes of the world soon after the appearance of  
653 terrestrial plants over 400 million years ago (Scott and Glasspool, 2006; Bowman et  
654 al., 2009). Fire emissions affect the Earth system in several important ways. First,  
655 chemical Firespecies emitted from fires-emissions are a key component of the global  
656 and regional carbon budgets (Bond-Lamberty et al., 2007; Ciais et al., 2013; Kondo et  
657 al., 2018), ~~and also~~ a major source of greenhouse gases (Tian et al., 2016), ~~and the~~  
658 largest contributor of primary carbonaceous aerosols globally (Andreae and Rosenfeld,  
659 2008; Jiang et al., 2016). Second, bBy changing the atmospheric composition, fire  
660 emissions ~~can have resultant effects on~~ affect the global and regional radiation  
661 balance and climate (Ward et al., 2012; Tosca et al. 2013; Jiang et al., 2016; Grandey  
662 et al., 2016; McKendry et al., 2019; Hamilton et al., 2018; Thornhill et al., 2018).  
663 Third, fire emissions change the terrestrial nutrient and carbon cycles through altering  
664 the deposition of nutrients (e.g., nitrogen, phosphorus), surface ozone concentration,  
665 and meteorological conditions, terrestrial nutrient and carbon cycles (Mahowald et

666 al., 2008; Chen et al., 2010; McKendry et al., 2019; Yue and Unger, 2018). In  
667 addition, they degrade and the air quality (Val Martin et al., 2015; Knorr et al., 2017),  
668 which poses a significant risk to a major human health ~~hazard~~ and has been  
669 estimated to result in at least ~165,000, and more likely ~339,000 pre-mature deaths  
670 per year globally (Johnston et al., 2012; Marlier et al., 2013; Lelieveld et al., 2015).

671 To date, only emissions from individual fires or small-scale fire complexes can  
672 be directly measured from ~~—laboratory experiments and~~ field campaigns and  
673 laboratory experiments (Andreae and Merlet, 2001; Yokelson et al., 2013; Stockwell  
674 et al., 2016; Andreae, 2019). Regionally and globally, fire emissions are often  
675 estimated based on satellite observations, fire proxy recordsies, and  
676 numericalnumerical models, even though some attempts have been made to bridge the  
677 gap between local observations and regional estimations using combinations of  
678 aircraft and ground based measurements from field campaigns (e.g., SAMBBA,  
679 ARCTAS), satellite-based inventories, and chemical transport models (e.g., Fisher et  
680 al., 2010; Reddington et al., 2019; Konovalov et al., 2018). ~~—~~ Satellite-based fire  
681 emission estimates are primarily derived from satellite observations of burned area,  
682 active fire counts, and/or fire radiative power, and are sometimes/~~or~~ constrained by  
683 satellite observations of aerosol optical depth (AOD), CO, or CO<sub>2</sub> (Wiedinmyer et al.,  
684 2011; Kaiser et al., 2012; Krol et al., 2013; Konovalov et al., 2014; Ichoku and Ellison,  
685 2014; Darmenov and da Silva, 2015; van der Werf et al., 2017; Heymann et al., 2017).  
686 S-Dataatellite-based fire emission estimates are available globally, but only cover only  
687 the present-day period, i.e. since 1997 for GFED and shorter periods for others.

688 Historical change of fire emissions has been inferred from a variety of proxies,  
689 such as —include ice-core records of— CH<sub>4</sub> (isotope  $\delta^{13}\text{C}$  from pyrogenic or  
690 biomass burning source), black carbon, levoglucosan, vallic acid, ammonium, and CO-  
691 concentration trapped in the air enclosed in ice cores (Ferretti et al., 2005; McCormell  
692 et al., 2007; Conedera et al., 2009; Wang et al., 2012; Zennaro et al., 2014), site-level  
693 sedimentary charcoal records (Marlon et al., 2008, 2016), visibility records (van  
694 Marle et al., 2017a), and fire-scar records (Falk et al. 2011)and aerosol indices-  
695 (Duncan et al., 2003). Fire proxies can be used to reconstruct fire emissions on a local  
696 to global scale and for time periods of decades to millennia and beyond~~These fire~~  
697 ~~proxies cover decades to millennia,~~ However, butthey are of limited spatial extent  
698 and, cannot be directly related—converted into emission amounts. Moreover,; —and-  
699 have large uncertainties and discrepancies were shown in their inferred regional or  
700 global long-term trends due to limited sample size and often unclear representative  
701 areas and time periods of fire emissions (Pechony and Shindell, 2010; van der Werf et  
702 al., 2013; Legrand et al., 2016).

703 Dynamic Global Vegetation Models (DGVMs) that include fire modeling are  
704 indispensable for estimating fire carbon emissions at globallocal toand globalregional  
705 scales and for the past, present, and future periods (Hantson et al., 2016). These  
706 models represent interactions among fire dynamics, biogeochemistry, biogeophysics,  
707 and vegetation dynamics at the land surface withinin a physically and chemically  
708 consistent modeling framework. DGVMs are alsooften constituteused as the terrestrial  
709 ecosystem component of Earth System models (ESMs) and have been widely applied

710 ~~in are applied to~~ global change research (Levis et al., 2004; Li et al., 2013; Kloster  
711 and Lasslop, 2017). ~~Using fire carbon emissions simulated by DGVMs and fire~~  
712 ~~emission factors,~~ fire emissions of trace gases and aerosols ~~can be can be~~ derived  
713 from the product of fire carbon emissions simulated by DGVMs and fire emission  
714 factors (Li et al., 2012; Knorr et al., 2016).

715 Modeling fire and fire emissions within DGVMs started in the early 2000s  
716 (Thonicke et al., 2001), and has rapidly progressed ~~during during~~ the past decade  
717 (Hantson et al., 2016). The Fire Model Intercomparison Project (FireMIP) initiated in  
718 2014 was the first international collaborative effort to better understand the behavior  
719 of global fire models (Hantson et al., 2016).; ~~A where a~~ set of common fire modeling  
720 experiments driven by the same forcing data were performed (Rabin et al., 2017).  
721 Nine DGVMs with different state-of-the-art global fire models participated in  
722 FireMIP. All global fire models used in the upcoming 6<sup>th</sup> Coupled Model  
723 Intercomparison Project (CMIP6) and IPCC AR6 ~~are were~~ included in FireMIP,  
724 except for the fire scheme in GFDL-ESM (Rabin et al., 2018; Ward et al., 2018)  
725 which is similar to that of CLM4.5 (Li et al., 2012) in FireMIP. ~~Furthermore, Note that~~  
726 GlobFIRM (Thonicke et al., 2001) in FireMIP ~~waiss~~ the most commonly-used fire  
727 scheme in CMIP5 (Kloster and Lasslop, 2017), and is still used by some models in  
728 CMIP6.

729 Earlier studies provided only one single time series of fire emissions for global  
730 grids or regions (Schultz et al., 2008; Mieville et al., 2010; Lamarque et al., 2010;  
731 Marlon et al., 2016; van Marle et al., 2017b; and references therein).; ~~This limit sing~~

732 their utility for quantifying the uncertainty in global and regional reconstructions of  
733 fire emissions and ~~its subsequent~~ the corresponding impacts on estimated historical  
734 changes in carbon cycle, climate, and air pollution. A small number of studies also  
735 investigated the drivers of fire carbon emission trends (Kloster et al., 2010; Yang et al.,  
736 2014; Li et al., 2018; Ward et al., 2018). However, ~~—because only a single DGVM~~  
737 ~~was used in these studies, they~~ these studies could not identify the uncertainty source  
738 in recent model-based reconstructions or help understand the inter-model discrepancy  
739 in projections of future fire emissions because only a single DGVM was used in each.

740 ~~Our study~~ This study provides a new dataset of global gridded fire emissions,  
741 including carbon and 33 species of trace gases and aerosols, over the 1700–2012 time  
742 period, based on ~~the~~ nine DGVMs with different state-of-the-art global fire models  
743 that participated in FireMIP. ~~The~~ The dataset provides ~~the~~ a basis for developing  
744 multi-source (e.g., satellite-based products, model simulations, and/or fire proxy  
745 records) merged fire emission reconstructions and methods. It also, for the first  
746 time, allows end users to select all or a subset of model-based reconstructions that best  
747 suits their regional or global research needs; ~~and~~ importantly, it enables to  
748 quantify the quantification of the uncertainty range of past fire emissions and their  
749 resulting impacts. In addition, the model-based estimates of fire emissions are  
750 comprehensively evaluated through comparison with satellite-based products,  
751 including amounts, spatial distribution, seasonality, and interannual variability, thus  
752 providing information on the limitations of recent model-based reconstructions. We  
753 also analyze the simulated long-term trends changes ~~—of the model-based~~

754 | ~~reconstructions, and the the forcing drivers of these trends~~ for each DGVM and ~~for~~  
755 | inter-model ~~diserepancy~~differences.

756

## 757 **2 Methods and datasets**

### 758 **2.1 Models in FireMIP**

759 Nine DGVMs with different fire modules participated in FireMIP: CLM4.5 with  
760 CLM5 fire module, CTEM, JSBACH-SPITFIRE, JULES-INFERNO,  
761 LPJ-GUESS-GlobFIRM, LPJ-GUESS-SIMFIRE-BLAZE, LPJ-GUESS-SPITFIRE,  
762 MC2, and ORCHIDEE-SPITFIRE (Table 1, see Rabin et al., 2017 for detailed  
763 description of each model). JSBACH, ORCHIDEE, and LPJ-GUESS used the  
764 variants of SPITFIRE (Thonicke et al., 2010) with updated representation of human  
765 ignition and suppression, fuel moisture, combustion completeness, and the  
766 relationship between spread rate and wind speed for JSBACH (Lasslop et al., 2014),  
767 combustion completeness for ORCHIDEE (Yue et al., 2014, 2015), and human  
768 ignition, post-fire mortality factors, and modifications for matching tree age/size  
769 structure for LPJ-GUESS (Lehsten et al., 2009; Rabin et al., 2017).

770 The global fire models in the nine DGVMs have diverse levels of complexity  
771 (Rabin et al., 2017). SIMFIRE is a statistical model based on present-day  
772 satellite-based fire products (Knorr et al., 2016). In CLM4.5, crop, peat, and tropical  
773 deforestation fires are empirically/statistically modeled (Li et al., 2013). The scheme  
774 for fires outside the tropical closed forests and croplands in CLM4.5 (Li et al., 2012;  
775 | Li and Lawrence, 2017) ~~and~~ , fire modules in CTEM (Arora and Boer, 2005; Melton

776 and Arora, 2016), GlobFIRM (Thonicke, 2001), and INFERNO (Mangeon et al., 2016)  
777 are process-based and of intermediate-complexity. That is, area burned is determined  
778 by two processes: fire occurrence and fire spread, but with simple empirical/statistical  
779 equations for each process. Fire modules in MC2 (Bachelet et al., 2015; Sheehan et al.,  
780 2015) and SPITFIRE variants are more complex, which use the Rothermel equations  
781 (Rothermel, 1972) to model fire spread and consider the impact of fuel composition  
782 on fire behavior.

783 ~~The way in which~~How humans affect fires ~~is treated differently~~differs among  
784 these global fire models (Table 2), ~~which influences~~ing their estimates ~~–simulations~~  
785 of fire emissions. GlobFIRM does not consider any direct human effect on fires, and  
786 MC2 fire model only considers human suppression on fire. CLM4.5 models fires in  
787 croplands, human deforestation and degradation fires in tropical closed forests, and  
788 human ignition and suppression for both occurrence and spread of fires outside of  
789 tropical closed forests and croplands.~~CLM4.5 includes crop fires, fires caused by~~  
790 ~~man-made deforestation in tropical closed forests, and human ignitions and~~  
791 ~~suppression on both fire occurrence and spread area for fires outside tropical closed~~  
792 ~~forests and croplands.~~–Burned area in SIMFIRE and human influence on fire  
793 occurrence in other models are a non-linear function of population density. CTEM  
794 and JSBACH-SPITFIRE also consider human suppression on fire duration.

795 JULES-INFERNO treats croplands and crop fires as natural grasslands and grassland  
796 fires. All models, except for CLM4.5 and INFERNO, set burned area to zero inever  
797 croplands. FireMIP mModels treat pasture fires as natural grassland fires by using the

798 same parameter values if they have pasture plant functional types (PFTs) or lumping  
799 pastures with natural grasslands otherwise. ~~Note that b~~Biomass harvest is considered  
800 in pastures in LPJ-GUESS-GlobFIRM and LPJ-GUESS-SIMFIRE-BLAZE, which  
801 decreases fuel availability for fires, and that JSBACH-SPITFIRE sets high fuel bulk  
802 density for pasture PFTs.

803 Only CLM4.5 simulates peat fires, although only emissions from burning of  
804 vegetation tissues and litter are included in outputs for FireMIP<sub>2</sub> (i.e., burning of soil  
805 organic matter is not included) (Table 2).

806 In the FireMIP models, fire carbon emissions are calculated as the product of  
807 burned area, fuel load, and combustion completeness. Combustion completeness is the  
808 fraction of live plant tissues and ground litter burned (~~0.0–100%.0~~). It depends on  
809 PFT and plant tissue type in GlobFIRM and in the fire modules of CLM4.5 and  
810 CTEM, and is also a function of soil moisture in INFERNO. Combustion  
811 completeness depends on plant tissue type and surface fire intensity in SIMFIRE, fuel  
812 type and wetness in the SPITFIRE family models, and fuel type, load, and moisture in  
813 MC2 fire module.

814

## 815 **2.2 FireMIP experimental protocol and input datasets**

816 The nine DGVMs in FireMIP are driven with the same forcing data (Rabin et al.,  
817 2017). The atmospheric forcing is from CRU-NCEP v5.3.2 with a spatial resolution of  
818 0.5° and a 6-hourly temporal resolution (Wei et al., 2014). The 1750–2012 annual  
819 global atmospheric CO<sub>2</sub> concentration is derived from ice core and NOAA monitoring

820 station data (Le Quéré et al., 2014). Annual land-use and land-cover change (LULCC)  
821 and population density at a 0.5° resolution for 1700–2012 are from Hurtt et al. (2011)  
822 and Klein Goldewijk et al. (2010, HYDE v3.1), respectively. Monthly  
823 cloud-to-ground lightning frequency for 1901–2012, at 0.5° resolution, is derived  
824 from the observed relationship between present-day lightning and convective  
825 available potential energy (CAPE) anomalies (Pfeiffer et al., 2013, J. Kaplan, personal  
826 communication, 2015).

827 Fire emissions in this study are estimated using the model outputs of PFT-level  
828 fire carbon emissions and vegetation characteristics (PFTs and their fractional area  
829 coverages) from the FireMIP historical transient control run (SF1) (Rabin et al., 2017).  
830 SF1 includes three phases (Fig. 1): the 1700 spin-up phase, the 1701–1900 transient  
831 phase, and the 1901–2012 transient phase. In the 1700 spin-up phase, all models are  
832 spun up to equilibrium, forced by population density and prescribed ~~land-use-and-~~  
833 ~~land-cover-change~~ (LULCC) at their 1700 values, 1750 atmospheric CO<sub>2</sub>  
834 concentration, and the repeatedly cycled 1901–1920 atmospheric forcing  
835 (precipitation, temperature, specific humidity, surface pressure, wind speed, and solar  
836 radiation) and lightning data. The 1701–1900 transient phase is forced by 1701–1900  
837 time-varying population and LULCC, with constant CO<sub>2</sub> concentration at 1750 level  
838 until 1750 and time-varying CO<sub>2</sub> concentration for 1750–1900, and the cycled  
839 1901–1920 atmospheric forcing and lightning data. In the 1901–2012 transient phase,  
840 models are driven by 1901–2012 time-varying population density, LULCC, CO<sub>2</sub>

841 concentration, atmospheric forcing, and lightning data. Unlike all other models, MC2  
842 and CTEM run from 1901 and 1861, respectively, rather than 1700.

843 ~~The nine DGVMs are driven with the same forcing data (Rabin et al., 2017). The~~  
844 ~~atmospheric forcing is from CRU-NCEP v5.3.2 with a spatial resolution of 0.5° and a~~  
845 ~~6-hourly temporal resolution (Wei et al., 2014). The 1750–2012 annual global~~  
846 ~~atmospheric CO<sub>2</sub> concentration is derived from ice core and NOAA monitoring~~  
847 ~~station data (Le Quéré et al., 2014). Annual LULCC and population density at a 0.5°~~  
848 ~~resolution for 1700–2012 are from Hurtt et al. (2011) and Klein Goldewijk et al.~~  
849 ~~(2010, HYDE v3.1), respectively. Monthly cloud-to-ground lightning frequency for~~  
850 ~~1901–2012, at 0.5° resolution, is derived from the observed relationship between~~  
851 ~~present-day lightning and convective available potential energy (CAPE) anomalies~~  
852 ~~(Pfeiffer et al., 2013, J. Kaplan, personal communication, 2015).~~

853 Six FireMIP models (CLM4.5, JSBACH-SPITFIRE, JULES-INFERNO,  
854 LPJ-GUESS-SPITFIRE, LPJ-GUESS-SIMFIRE-BLAZE, and  
855 ORCHIDEE-SPITFIRE) also provide outputs of five sensitivity simulations: constant  
856 climate, constant atmospheric CO<sub>2</sub> concentration, constant land cover, constant  
857 population density, and constant lightning frequency throughout the whole simulation  
858 period. The sensitivity simulations are helpful for understanding the drivers of  
859 changes in reconstructed fire emissions.

860

### 861 **2.3 Estimates of fire trace gas and aerosol emissions**

862 Based on fire carbon emissions and vegetation characteristics from DGVMs and fire  
863 emission factors, fire emissions of trace gas and aerosol species  $i$  and the PFT  $j$ ,  $E_{ij}$  (g  
864 species  $\text{m}^{-2} \text{s}^{-1}$ ), are estimated according to Andreae and Merlet (2001):

$$865 \quad E_{ij} = EF_{ij} \times CE_j / [C], \quad (1)$$

866 where  $EF_{ij}$  (g species (kg dry matter (DM)) $^{-1}$ ) is a PFT-specific emission factor (EF),  
867  $CE_j$  denotes the fire carbon emissions of PFT  $j$  (g C  $\text{m}^{-2} \text{s}^{-1}$ ), and  $[C]=0.5 \times 10^3$  g C (kg  
868 DM) $^{-1}$  is a unit conversion factor from carbon to dry matter.

869 The EFs used in this study (Table 3) are based on Andreae and Merlet (2001),  
870 with updates from field and laboratory studies over various land cover types published  
871 during 2001–2018 (~~see Andreae, \_\_ (2019) for details~~2019). All FireMIP model  
872 simulations used the same EFs from Table 3. The EFs are used for all simulations of  
873 FireMIP models in the present study.

874 DGVMs generally simulate vegetation as mixture of PFTs in a given grid  
875 location to represent plant function at global scale, instead of land cover types. In  
876 Table 4, we associate the PFTs from each DGVM to the land cover types shown in  
877 Table 3. Grass, shrub, savannas, woodland, pasture, tundra PFTs are classified as  
878 grassland/savannas; ~~Tree~~ PFTs and crop PFTs are classified as forests and ~~crop~~  
879 PFTs as croplands, respectively, similar to Li et al. (2012), Mangeon et al. (2016), and  
880 Melton and Arora (2016). PFTs of evergreen tree and other broadleaf deciduous tree  
881 in CTEM, extra-tropical evergreen and deciduous tree in JSBACH, and broadleaf  
882 deciduous tree and needleleaf evergreen tree in JULES are divided into tropical,  
883 temperate, and boreal groups following Nemani and Running (1996).

884 We provide two versions of fire emission products with different spatial  
885 resolutions: the original spatial resolution for each FireMIP DGVM outputs (Table 1),  
886 and a 1x1 degree horizontal resolution. For the latter, fire emissions are unified to 1  
887 degree resolution using bilinear interpolation for CLM4.5, CTEM, JSBACH, and  
888 JULES which have coarser resolution, and area-weighted averaging-up for other  
889 models whose original resolution is 0.5 degree. The 1x1 degree product is used for  
890 present-day evaluation and historical trend analyses in Sects. 3 and 4.

891

## 892 **2.4 Benchmarks**

893 Satellite-based products are commonly used as benchmarks to evaluate present-day  
894 fire emission simulations (Rabin et al., 2017, and references therein). In the present  
895 study, six satellite-based products are used (Table 5). Fire emissions in  
896 GFED4/GFED4s (small fires included in GFED4s) (van der Werf et al., 2017),  
897 GFAS1.2 (Kaiser et al., 2012), and FINN1.5 (Wiedinmyer et al., 2011) are based on  
898 emission factor (EF) and fire carbon emissions (CE) (Eq. 1). CE is estimated from  
899 MODIS burned area and VIRS/ATSR active fire products in the GFED family,  
900 MODIS active fire detection in FINN1.5, and MODIS fire radiative power (FRP) in  
901 GFAS1. Fire emissions from FEER1 (Ichoku and Ellison, 2014) and QFEDv2.5  
902 (Darmenov and da Silva, 2015) are derived using FRP, and constrained with satellite  
903 AOD observations. Satellite-based present-day fire emissions for the same region can  
904 differ by a factor of 2–4 on an annual basis (van der Werf et al., 2010) and up to 12 on  
905 a monthly basis (Zhang et al., 2014). The discrepancy among satellite-based estimates

906 of present-day fire emissions them mainly comes from the satellite observations used,  
907 the methods applied for deriving fire emissions, and the emissions factors.

908

## 909 **2.5 Multi-source merged historical reconstructions**

910 We also compared the simulated historical changes with historical reconstructions  
911 merged from multiple sources used as forcing data for CMIPs. Fire emission estimates  
912 for CMIP5 and CMIP6 were merged from different sources (Table 5). For CMIP5  
913 (Lamarque et al., 2010), the decadal fire emissions are available from 1850 to 2000,  
914 estimated using GFED2 fire emissions (van der Werf et al., 2006) for 1997 onwards,  
915 RETRO (Schultz et al., 2008) for 1960–1900, GICC (Mieville et al., 2010) for  
916 1900–1950, and kept constant at the 1900 level for 1850–1900. RETRO combined  
917 literature reviews with satellite-based fire products and the GlobFIRM fire model.  
918 GICC is based on a burned area reconstruction from literature review and sparse tree  
919 ring records (Mouillot et al., 2005), satellite-based fire counts, land cover map, and  
920 representative biomass density and burning efficiency of each land cover type.

921 For CMIP6, monthly fire emission estimates are available from 1750 to 2015  
922 (van Marle et al., 2017b). The CMIP6 estimates are merged from GFED4s fire carbon  
923 emissions for 1997 onwards, charcoal records GCDv3 (Marlon et al., 2016) for North  
924 America and Europe, visibility records for Equatorial Asia (Field et al., 2009) and  
925 central Amazon (van Marle et al., 2017b), and the median of simulations of six  
926 FireMIP models (CLM4.5, JSBACH-SPITFIRE, JULES-INFERNO,  
927 LPJ-GUESS-SPITFIRE, \_\_\_\_\_LPJ-GUESS-SIMFIRE-BLAZE, and

928 ORCHIDEE-SPITFIRE) for all other regions. Then, based on the merged fire carbon  
929 emissions, CMIP6 fire trace gas and aerosols emissions are derived using EF from  
930 Andreae and Merlet (2001) with updates to 2013 and Akagi et al. (2011) with updates  
931 for temperate forests to 2014, and a present-day land cover map.

932

### 933 **3 Evaluation of present-day fire emissions**

934 The spatial pattern and temporal variability of different fire emission species are  
935 similar, with ~~some slight differences~~ ~~diserepancies~~ resulting from the estimated fire  
936 carbon emissions ~~from over~~ the land cover types that have different emission factors  
937 (Table 3). Therefore, we focus on several important species as examples to exhibit the  
938 performance of FireMIP models on the simulations of present-day fire emissions.

939

#### 940 **3.1 Global amounts and spatial distributions**

941 As shown in Table 6, FireMIP models, except for MC2 and LPJ-GUESS-GlobFIRM,  
942 estimate present-day fire carbon, CO<sub>2</sub>, CO, CH<sub>4</sub>, BC, OC, and PM<sub>2.5</sub> annual emissions  
943 to be within the range of satellite-based products. For example, the estimated range of  
944 fire carbon emissions is 1.7–3.0 Pg C yr<sup>-1</sup>, whereas ~~they are it is~~ 1.5–4.2 Pg C yr<sup>-1</sup> for  
945 satellite-based products. Low fire emissions in MC2 result from relatively low  
946 simulated global burned area, only about 1/4 of satellite-based observations (Andela  
947 et al., 2017). ~~In contrast, whereas~~ high emissions in LPJ-GUESS-GlobFIRM are  
948 mainly due to the higher combustion completeness of woody tissues (~~70–~~90% of  
949 stem and coarse woody debris burned in post-fire regions) than those used in other

950 FireMIP models ([Table 2](#))[Rabin et al., 2017](#)) and the satellite-based GFED family  
951 ([20–40% for stem and 40–60% for coarse woody debris](#)) ([van der Werf et al., 2017](#)).

952 FireMIP DGVMs, except for MC2, represent the general spatial distribution of  
953 fire emissions evident in satellite-based products, with high fire BC emissions over  
954 tropical savannas and low emissions over the arid and sparsely vegetated regions (Fig.  
955 2). Among the nine models, CLM4.5, JULES-INFERNO, and  
956 LPJ-GUESS-SIMFIRE-BLAZE have higher global spatial pattern correlation with  
957 satellite-based products than the other models, indicating higher skill in their  
958 spatial-pattern simulations. It should also be noted that, on a regional scale, CTEM,  
959 JULES-INFERNO, LPJ-GUESS-SPITFIRE, and ORCHIDEE-SPITFIRE  
960 underestimate fire emissions over boreal forests in Asia and North America.  
961 LPJ-GUESS-GlobFIRM and LPJ-GUESS-SIMFIRE-BLAZE overestimate fire  
962 emissions over the Amazon and African rainforests. CLM4.5 and  
963 ~~JSBACH-SPITFIRE~~[LPJ-GUESS-GlobFIRM](#) overestimate fire emissions over eastern  
964 China ~~and North America, respectively.~~ [JSBACH-SPITFIRE underestimates fire](#)  
965 [emissions in most tropical forests.](#) MC2 underestimates fire emissions over most  
966 regions, partly because it allows only one ignition per year per grid cell and thus  
967 underestimates the burned area.

968 We further analyze the spatial distribution of inter-model differences. As shown  
969 in Fig. 3, the main disagreement among FireMIP models occurs in the tropics,  
970 especially over the tropical savannas in Africa, South America, and northern Australia.  
971 [This is mainly driven by the MC2, CTEM, JSBACH-SPITFIRE, and](#)

972 ORCHIDEE-SPITFIRE simulations (Fig. 2). Differences among the satellite-based  
973 estimates have a similar spatial pattern, but higher than the inter-model spread in  
974 savannas over southern Africa and lower in the temperate arid and semi-arid regions  
975 and north of 60°N over Eurasia (Fig. S1a).

### 977 **3.2 Seasonal cycle**

978 The FireMIP models reproduce similar seasonality features of fire emissions to  
979 satellite-based products, that is, peak month is varied from the dry season in the  
980 tropics to the warm season in the extra-tropics (Fig. 4).

981 For the tropics in the Southern Hemisphere, fire PM<sub>2.5</sub> emissions of  
982 satellite-based products peak in August–September. Most FireMIP models can  
983 reproduce this pattern, except ORCHIDEE-SPITFIRE and LPJ-GUESS-SPITFIRE  
984 peaking two months and one month earlier, respectively, and JSBACH-SPITFIRE  
985 with much lower amplitude of seasonal variability likely caused by parameter setting  
986 in its fuel moisture functions (Table S9 in Rabin et al. (2017)6).

987 For the tropics in the Northern Hemisphere, most FireMIP models exhibit larger  
988 fire emissions in the northern winter, consistent with the satellite-based products.

989 In the northern extra-tropical regions, satellite-based products show two periods  
990 of high values: April–May resulting mainly from fires inover croplands and  
991 grasslands, and July mainly due to fires inover the boreal evergreen forests. Most  
992 FireMIP models can reproduce the second one, except for LPJ-GUESS-SPITFIRE

993 which peaks in October. CLM4.5 is the only model that can captures both peak  
994 periods partly because it's the only one to model the crop fires.

995

### 996 **3.3 Interannual variability**

997 Global fire PM<sub>2.5</sub> emissions from satellite-based products for 1997–2012 show a  
998 substantial interannual variability, which peaks in 1997–1998, followed by a low  
999 around 2000 and a decline starting in 2002–/2003 (Fig. 5). The 1997–1998 high  
1000 emission values are caused by peat fires in Equatorial Asia in 1997 and widespread  
1001 drought-induced fires in 1998 associated with the most powerful ~~1997–1998~~-El Niño  
1002 event in 1997–1998 recorded in history (van der Werf et al., 2017; Kondo et al., 2018).  
1003 Most FireMIP models cannot reproduce the 1997–1998 peak, except for CLM4.5 as  
1004 the only model that simulates the burning of plant-tissue and litter from peat fires  
1005 (although burning of soil organic matter is not included) and the drought-linked  
1006 tropical deforestation and degradation fires (Li et al., 2013, Kondo et al., 2018).  
1007 CLM4.5, CTEM, and LPJ-GUESS-SIMFIRE-BLAZE present the highest temporal  
1008 correlation between models and satellite-based products (0.55–0.79 for CLM4.5,  
1009 0.51–0.68 for CTEM, and 0.39–0.72 for LPJ-GUESS-SIMFIRE-BLAZE), and thus  
1010 are more skillful than other models to reproduce the interannual variability observed  
1011 from satellite-based products (Table 7).

1012 We use the coefficient of variation (CV, the standard deviation divided by the  
1013 mean, %) to represent the amplitude of interannual variability of fire emissions. As  
1014 shown in Fig. 5, for 1997–2012, all FireMIP models underestimate the variation as a

1015 result of (at least) partially missing the 1997–1998 fire emission peak. For 2003–2012  
1016 (the common period of all satellite-based products and models), interannual variation  
1017 of annual fire PM<sub>2.5</sub> emissions in CLM4.5, CTEM, and LPJ-GUESS family models  
1018 lies within the range of satellite-based products (CV=6–12%). Other models present  
1019 weaker variation (CV=5%) except for MC2 (CV=24%) that has a much stronger  
1020 variation than all satellite-based products and other FireMIP models.

1021

## 1022 **4 Historical changes and drivers**

### 1023 **4.1 Historical changes ~~and drivers~~**

1024 Figure 6 shows historical simulations of the FireMIP models and the CMIP  
1025 reconstructions for fire carbon, CO<sub>2</sub>, CO<sub>2</sub> and PM<sub>2.5</sub> emissionspecies. We find similar  
1026 historical changes for all the species, with the maximum global fire emissions given  
1027 by LPJ-GUESS-GlobFIRM and the minima by LPJ-GUESS-SPITFIRE before 1901  
1028 and MC2 afterwards.

1029 Long-term trends in ~~modelled~~simulated global fire emissions for all models are  
1030 weak before the 1850s (relative trend <0.015% yr<sup>-1</sup>); They are similar to CMIP6  
1031 estimates (Fig. 6); but in disagreement with earlier reconstructions based on charcoal  
1032 records (Marlon et al., 2008; Marlon et al., 2016), ice-core CO records (Wang et al.,  
1033 2010), and ice-core δ<sup>13</sup>CH<sub>4</sub> records (Ferretti et al., 2005), which exhibit a rapid  
1034 increase from 1700 to roughly the 1850s.

1035 —

1036 After the 1850s, disagreement in the trends among FireMIP models begins to  
1037 emerge. Fire emissions in LPJ-GUESS-SIMFIRE-BLAZE decline since ~1850, while  
1038 fire emissions in LPJ-GUESS-SPITFIRE, MC2, and ORCHIDEE-SPITFIRE show  
1039 upward trends from ~1900s. In CLM4.5, CTEM, and JULES-INFERNO, fire  
1040 emissions increase slightly before ~1950, similar to the CMIP6 estimates, but CTEM  
1041 and JULES-INFERNO decrease thereafter, contrary to CMIP5 and CMIP6 estimates  
1042 and CLM4.5. JSBACH-SPITFIRE simulates a decrease of fire emissions before  
1043 1940s and an increase later, similar to the CMIP5 estimates. All the long-term trends  
1044 described above are significant at the 0.05 level using the Mann-Kendall trend test.

1045 ~~—Six FireMIP models also conducted sensitivity experiments, which can be~~  
1046 ~~used to identify the drivers of their long-term trends during the 20<sup>th</sup> century. As shown~~  
1047 ~~in Figs. 6 and 7, the downward trend of LPJ-GUESS-SIMFIRE-BLAZE is mainly~~  
1048 ~~caused by LULCC and increasing population density. Upward trends in~~  
1049 ~~LPJ-GUESS-SPITFIRE and ORCHIDEE-SPITFIRE are dominated by LULCC and~~  
1050 ~~rising population density and CO<sub>2</sub> during the 20<sup>th</sup> century. In CLM4.5 and~~  
1051 ~~JULES-INFERNO, upward trends before ~1950 are attributed to rising CO<sub>2</sub>, climate~~  
1052 ~~change, and LULCC, and the subsequent drop in JULES-INFERNO mainly results~~  
1053 ~~from the rising population density and climate change. Long-term changes in~~  
1054 ~~JSBACH-SPITFIRE are mainly driven by LULCC and rising CO<sub>2</sub>.—~~

1055 Earlier reconstructions based on fire proxies also show a big difference in  
1056 long-term changes after the 1850s. The reconstruction based on the Global Charcoal  
1057 Database version 3 (GCDv3, Marlon et al., 2016) exhibits a decline from the late 19<sup>th</sup>

1058 century to the 1920s, and then an upward trend until ~1970, followed by a drop. The  
1059 reconstructions based on the GCDv1 (Marlon et al., 2008) and ice-core CO records  
1060 (Wang et al., 2010) show a sharp drop since roughly the 1850s, while a steady rise is  
1061 exhibited in the reconstruction based on ice-core  $\delta^{13}\text{CH}_4$  records (Ferretti et al., 2005).  
1062 The simulated historical changes of FireMIP models (Fig. 6) fall into this fairly broad  
1063 range of long-term trends in these reconstructions.

1064 Spatial patterns of inter-model spread of fire emissions for 1700–1850 and  
1065 1900–2000 (Figs. S1b–c) are similar to the present-day patterns as shown in Fig. 3.

1066

## 1067 **4.2 Drivers**

1068 Six FireMIP models also conducted sensitivity experiments, which can be used to  
1069 isolate the role of individual forcing factors in long-term trends of fire emissions  
1070 during the 20th century. The median of the six models are also used for building  
1071 CMIP6 fire emission estimates (van Marle et al. 2017b). The 20th century changes of  
1072 driving forces used in FireMIP are characterized by an increase in the global land  
1073 temperature, precipitation, lightning frequency, atmospheric CO<sub>2</sub> concentration,  
1074 population density, cropland and pasture areas, and a decrease in the global forest area  
1075 (Teckentrup et al., 2019).

1076 As shown in Figs. 6 and 7, the downward trend of global fire emissions in  
1077 LPJ-GUESS-SIMFIRE-BLAZE is mainly caused by LULCC and increasing  
1078 population density. Upward trends in LPJ-GUESS-SPITFIRE and  
1079 ORCHIDEE-SPITFIRE are dominated by LULCC and rising population density and

1080 CO<sub>2</sub> during the 20th century. In CLM4.5 and JULES-INFERNO, upward trends  
1081 before ~1950 are attributed to rising CO<sub>2</sub>, climate change, and LULCC, and the  
1082 subsequent drop in JULES-INFERNO mainly results from the rising population  
1083 density and climate change. Long-term changes of global fire emissions in  
1084 JSBACH-SPITFIRE are mainly driven by LULCC and rising CO<sub>2</sub>. ~~for difference in~~  
1085 simulated long-term changes

1086 As shown in Fig. 7, t~~he~~ discrepancy/inter-model spread in long-term trends-  
1087 ~~among FireMIP models~~ mainly arises from the simulated anthropogenic influence  
1088 (LULCC and population density change) on fire emissions (~~Fig. 7~~), as the standard  
1089 deviation in simulated responses to LULCC (0.27 Pg C yr<sup>-1</sup>) and population density  
1090 (0.11 Pg C yr<sup>-1</sup>) is much larger than the other drivers.

1091 LULCC decreases global fire emissions sharply in  
1092 LPJ-GUESS-SIMFIRE-BLAZE during the 20th century, but increases global fire  
1093 emissions for the other models except for JSBACH-SPITFIRE. The response to  
1094 LULCC in LPJ-GUESS-SIMFIRE-BLAZE is because it assumes no fire in croplands  
1095 and accounts for biomass harvest (~~((thus decreases/reducing~~es fuel availability)) in  
1096 pastures (Table 2), the area of which expanded over the 20th century. The  
1097 LULCC-induced increase in fire emissions for ~~the other-~~  
1098 ~~models~~ORCHIDEE-SPITFIRE, LPJ-GUESS-SPITFIRE, and JULES-INFERNO are  
1099 partly caused by increased burned area due to the expansion of grasslands (pastures  
1100 are lumped in natural grasslands in these models) where fuels are easier to burn than  
1101 woody vegetation in the model ~~setups of all FireMIP models~~ (Rabin et al., 2017).

1102 ~~Additionally,~~ CLM4.5 models crop fires and tropical deforestation and degradation  
1103 fires. ~~Crop fire emissions in CLM4.5~~ which are estimated to increase during the 20th  
1104 century due to expansion of croplands and increased fuel loads over time (Fig. S2).  
1105 Emissions of tropical deforestation and degradation fires in CLM4.5 are increased  
1106 before ~1950, responding to increased human deforestation rate in tropical closed  
1107 forests based on prescribed land use and land cover changes (Li et al. 2018). JSBACH  
1108 ~~shifts the sign of response to LULCC around ~1940s due to both assuming no fires~~  
1109 ~~over croplands and setting high fuel bulk density for pastures.~~ In JSBACH-SPITFIRE,  
1110 as croplands and pastures expand over time, the assumption of no fire over croplands  
1111 tends to decrease fire emissions, while the setting of high fuel bulk density for  
1112 pastures tends to increase fire emissions due to increased fuel combusted per burned  
1113 area, which together partly result in the shifted sign of response to LULCC around the  
1114 1940s.

1115 Rising population density throughout the 20th century decreases fire emissions in  
1116 CLM4.5 and LPJ-GUESS-SIMFIRE-BLAZE because they include human  
1117 suppression on both fire occurrence and fire spread. Fire suppression increases with  
1118 rising population density simulated explicitly in CLM4.5 and implicitly in  
1119 LPJ-GUESS-SIMFIRE-BLAZE. On the contrary, rising population density increases  
1120 fire emissions in LPJ-GUESS-SPITFIRE and ORCHIDEE-SPITFIRE because  
1121 observed human suppression on fire spread found in Li et al. (2013), Hantson et al.  
1122 (2015), and Andela et al. (2017) is not taken into account in the two models. The  
1123 response to population density change for the other models is small, reflecting the

1124 compensating effects of human ignition and human suppression on fire occurrence  
1125 (strongest in JULES-INFERNNO in FireMIP models), and also human suppression on  
1126 fire duration (JSBACH-SPITFIRE).

1127 All models simulate increased fire emissions with increased CO<sub>2</sub> since elevated  
1128 CO<sub>2</sub> increases fuel load through increasing the carbon entering into the land  
1129 ecosystems (Mao et al., 2009) and improving the water-use efficiency (Keenan et al.,  
1130 2013). Such a CO<sub>2</sub>-driven increase of fuel load is consistent with a recent analysis of  
1131 satellite-derived vegetation indices (Zhu et al., 2016). FireMIP models also agree that  
1132 impacts of changes in lightning frequency on long-term trends of fire emissions are  
1133 small. Moreover, most FireMIP models agree that climate change tends to increase  
1134 fire carbon emissions during the first several decades and then falls, reflecting  
1135 co-impacts of climate on both fuel load and fuel moisture.

1136

### 1137 **4.3 Regional long-term changes**

1138 We divided the global map into 14 regions following the definition of the GFED  
1139 family (Fig. 8a). As shown in Fig. 8b, inter-model discrepancy in long-term changes  
1140 are largest in Southern Hemisphere South America (SHSA), southern and northern  
1141 Africa (NHAF and SHAF), and central Asia (CEAS). ~~In other regions, long-term~~  
1142 ~~changes of most FireMIP models are small, similar to CMIP5 or CMIP6 fire emission~~  
1143 ~~estimates, except for equatorial Asia where only CLM4.5 partly reproduces the~~  
1144 ~~upward trend shown in CMIP5 and CMIP6 estimates after 1950s (not shown).~~

1145 Most FireMIP models reproduce the upward trends of fire CO emissions found  
1146 also in the CMIP5 or CMIP6 estimates since 1950s in SHSA and till ~1950 in Africa  
1147 (Figs. 9a, h, and i). Long-term trends in regional fire emissions in SHSA, Africa,  
1148 and central Asia can broadly explain the upward trends in global fire emissions in  
1149 LPJ-GUESS-SPITFIRE, MC2, and ORCHIDEE-SPITFIRE, the downward trends in  
1150 LPJ-GUESS-SIMFIRE-BLAZE, and the rise followed by a drop in CTEM, whose  
1151 global fire emissions exhibit most obvious long-term trends in FireMIP models (Fig.  
1152 6).

1153 In other regions, the difference in long-term changes among models is smaller  
1154 (Fig. 8b). Emissions of most models and CMIP5 estimates exhibit a significant  
1155 decline in temperate North America (TENA) from ~1850 to ~1970, while historical  
1156 changes of CMIP6 estimates are comparatively small (Fig. 9b).  
1157 LPJ-GUESS-SIMFIRE-BLAZE has a more obvious long-term change than the other  
1158 FireMIP models and CMIPs in boreal North America (BONA) and northern South  
1159 America (NHSA) (Figs. 9a and d). MC2 and LPJ-GUESS-GlobFIRM emissions  
1160 increase after ~1900 in Europe (EURO), while emissions of other models and CMIPs  
1161 are overall constant (Fig. 9f). In boreal Asia (BOAS), emissions of most models and  
1162 CMIP6 are relatively constant, while LPJ-GUESS-GlobFIRM and CMIP5 emissions  
1163 decline from 1850 to the 1950s and from 1900 to the 1970s, respectively, and then  
1164 rise (Fig. 9j). JULES, LPJ-GUESS-SIMFIRE-BLAZE, CLM4.5, CTEM, and CMIP6  
1165 emissions significantly decline since the 1950s in Southeast Asia (SEAS), while  
1166 CMIP5 emissions increase (Fig. 9l). In equatorial Asia (EQAS), CMIPs emissions

1167 increase after ~1950, which is partly reproduced by only CLM4.5 in FireMIP in  
1168 FireMIP only CLM4.5 partly reproduces it (Fig. 9m).

1169 As shown in Figs. S3–5, long-term changes of regional fire emissions for other  
1170 species are similar to those of fire CO emissions.

1171 The long-term changes of regional fire emissions and inter-model disagreement  
1172 are mainly caused by simulated responses to LULCC and/or population density  
1173 change for the 20th century (Figs. S6–19). Besides, climate change also plays an  
1174 important role in North America, northern South America, Europe, northern Africa,  
1175 boreal and central Asia, and Australia. FireMIP models generally simulate increased  
1176 regional fire emissions with increased CO<sub>2</sub> concentration and negligible impacts due  
1177 to changes in lightning frequency, similar to the responses of global fire emissions.

1178

1179

## 1180 **5 Summary and outlook**

1181 Our study provides the first<sup>new</sup> multi-model reconstructions of global historical fire  
1182 emissions for 1700–2012, including carbon and 33 species of trace gases and aerosols.

1183 Two versions of the fire emission product are available, at the original spatial  
1184 resolution for outputs of each FireMIP model and at on a unified 1x1 degree. The  
1185 dataset is based on simulations of fire carbon emissions and vegetation distribution  
1186 from nine DGVMs with state-of-the-art global fire models that participated in  
1187 FireMIP and the most up-to-date emission factors over various land cover types. It

1188 will be available to the public at

1189 <https://bwfilestorage.lsd.fkit.edu/public/projects/imk-ifu/FireMIP/emissions>.

1190 Our study provides an important dataset with wide-ranging applications for ~~the~~  
1191 ~~fire—and—the~~ Earth science research community~~ies~~. First, it is the first  
1192 multi-model-based reconstruction of fire emissions, and can serve as ~~thea~~ basis for  
1193 further develop~~ingment of~~ multi-source merged products of global and regional fire  
1194 emissions and ~~of~~ the merging methodology ~~itself~~. van Marle et al. (2017b) presented  
1195 an example for using part of the dataset to develop a multi-source merged fire  
1196 emission product as forcing dataset for CMIP6. In van Marle et al. (2017b), the  
1197 median of fire carbon emissions from six FireMIP models was used to determine  
1198 historical changes over most regions of the world. The merging method and merged  
1199 product in van Marle et al. (2017b) are still preliminary, and need to be improved in  
1200 the future, ~~e.g. e.g.~~ by weighting the different models depending on their global or  
1201 regional simulation skills. Secondly, our dataset includes global gridded  
1202 reconstructions for 300 years. ~~It can,~~ thus ~~be—can—be~~ used for analyzing global and  
1203 regional historical changes in fire emissions on inter-annual to multi-decadal time  
1204 scales and their interplay with climate variability and human activities. Third, the fire  
1205 emission reconstructions based on multiple models provide, for the first time, a  
1206 chance to quantify and understand the uncertainties in historical changes of fire  
1207 emissions and their subsequent impacts on carbon cycle, radiative balance, air quality,  
1208 and climate. Hamilton et al. (2018), for example, ~~usinged~~ fire emission simulations  
1209 from two global fire models and the CMIP6 estimates to drive an aerosol model, ~~. This~~

1210 ~~allowed for~~ —~~quantificatio~~~~ned~~ ~~of~~ the impact of uncertainties in pre-industrial fire  
1211 emissions ~~in~~~~on~~ estimated pre-industrial aerosol concentrations and historical radiative  
1212 forcing.

1213 This study also provides significant information of the recent state of fire model  
1214 performance by evaluating the present-day estimates based on FireMIP fire models  
1215 (also those used in the upcoming CMIP6). Our results show that most FireMIP  
1216 models can overall reproduce the amount, spatial pattern, and seasonality of fire  
1217 emissions shown by satellite-based fire products, ~~but~~~~Yet they~~ fail to simulate the  
1218 interannual variability partly due to a lack of modeling peat and tropical deforestation  
1219 fires. In addition, Teckentrup et al. (2019) found that climate was the main driver of  
1220 interannual variability for the FireMIP models. ~~a~~ good representation of fire  
1221 duration may be important to get the ~~variable~~-response of fire emissions to climate  
1222 right. ~~Teckentrup et al. (in prep.) found that climate greatly affected interannual~~  
1223 ~~variability of burned area partly through affecting fire duration.~~ —However, all  
1224 FireMIP models limit the ~~ir~~ fire duration of individual fire events no more than~~within~~  
1225 one day ~~in~~~~over~~ natural vegetation regions, so they cannot skillfully model the  
1226 drought-induced large fires that last multiple days (Le Page et al., 2015; Ward et al.,  
1227 2018). Recently, Andela et al. (20198) derived a dataset of fire duration from MODIS  
1228 satellite observations, which provides~~ed~~ a valuable dataset for developing  
1229 parameterization of fire duration in global fire models.

1230 This study also identifies population density and LULCC as the primary  
1231 uncertainty sources in fire emission estimates. Therefore, accurately modeling the

1232 responses to these responses remains a top priority forte reducinge uncertainty in  
1233 historical reconstructions and future projections of fire emissions, especially given  
1234 that modeling is the only way for future projections. For the response to changes in  
1235 population density, many FireMIP models have not included the observed relationship  
1236 between population density and fire spread (Table 2). Moreover, Bistinas et al. (2014)  
1237 and Parisien et al. (2016) reported obvious spatial heterogeneity of the population  
1238 density–burned area relationship that is poorly represented in FireMIP models.

1239 For the response to LULCC, improving the modeling of crop fires, and pasture  
1240 fires, deforestation and degradation fires, and human indirect effect on fires (e.g. e.g.,  
1241 fragmentation of the landscape) and reducing the uncertainty in the interpretation of  
1242 land use data set in models are critical. Fire has been widely used in agricultural  
1243 management during the harvesting, post-harvesting, or pre-planting periods (Korontzi  
1244 et al., 2006; Magi et al., 2012). Crop fire emissions are an important source of  
1245 greenhouse gases and air pollutants (Tian et al., 2016; Wu et al., 2017; Andreae,  
1246 2019). GFED4s reported that fires in croplands can contribute 5% of burned area and  
1247 6% of fire carbon emissions globally in the present day (Randerson et al., 2012; van  
1248 der Werf et al., 2017). In FireMIP, only CLM4.5 simulates crop fires, whereas the  
1249 other models assume no fire in croplands or treat croplands as natural grasslands. In  
1250 CLM4.5, crop fires contribute 5% of the global burned area in 2001–2010, similar to  
1251 GFED4s estimates. However, CLM4.5 estimates a total of 260 Tg C yr<sup>-1</sup> carbon  
1252 emissions (contribution rate:13%), which is higher than the GFED4s estimate (138 Tg  
1253 C yr<sup>-1</sup>) because CLM4.5 simulates higher fuel loads in croplands than the CASA

1254 model used by GFED4s. In CLM4.5, both the carbon emissions from crop fires and  
1255 the contribution of crop fire emissions to the total fire emissions increase throughout  
1256 the 20th century (Fig. S2), which is consistent with earlier estimates based on a  
1257 different crop fire scheme (Ward et al., 2018). In JULES-INFERNO, an increase in  
1258 cropland area also leads to an increase in burned area and fire carbon emissions  
1259 because this model treats croplands as natural grasslands. Grasses dry out faster than  
1260 woody vegetation and are easier to burn, so an increasing cropland area leads to  
1261 increasing burned area and fire carbon emissions. On the other hand, for FireMIP  
1262 models that exclude croplands from burning, expansion of croplands leads to a  
1263 decrease in burned area and fire carbon emissions. Therefore, different treatment of  
1264 crop fires can contribute to the uncertainty in simulated fire emissions. Since four out  
1265 of six FireMIP models used for generating CMIP6 estimates exclude croplands from  
1266 burning (van Marle et al., 2017b), CMIP6 estimates may underestimate the impact of  
1267 historical changes of crop fire emissions in some regions (e.g., China, Russia, India).  
1268 Given the small extent of crop fires, high resolution remote sensing may help improve  
1269 the detection of crop fires (Randerson et al., 2012; Zhang et al., 2018), which can  
1270 benefit the driver analyses and modeling of historical crop fires and their emissions in  
1271 DGVMs. Earlier studies reported that the timing and emissions from crop fires were  
1272 different from natural vegetation fires, and that crop fires could be an important  
1273 source of greenhouse gas and air pollutant emissions (Magi et al., 2012; Tian et al.,  
1274 2016; Wu et al., 2017). In FireMIP, only CLM4.5 simulates crop fires, whereas the  
1275 other models assume no fire over croplands.

1276 Le Page et al. (2017) and Li et al. (2018) highlighted the importance of  
1277 tropical deforestation and degradation fires in the long-term changes of reconstructed  
1278 and projected global fire emissions, but in FireMIP only CLM4.5 estimates the  
1279 tropical deforestation and degradation fires. For pasture fires, all FireMIP models  
1280 assume that they ~~behave like~~ are as natural grassland fires, ~~which~~ and this needs to be  
1281 verified by, for example, satellite-based products. If fires over pastures and natural  
1282 grasslands are significantly different, adding the gridded coverage of pasture as a new  
1283 input field in DGVMs without pasture PFTs and developing a parameterization of  
1284 pasture fires will be necessary. ~~In addition~~ Furthermore, Archibald (2016) and Andela  
1285 et al. (2017) found that expansion of croplands and pastures decreased fuel continuity  
1286 and thus reduced burned area and fire emissions. However, no FireMIP model  
1287 parameterizes this indirect human effect on fires. In addition, DGVMs generalize the  
1288 global vegetation using different sets of PFTs (Table 4) and represent land use data in  
1289 different way. This may lead to different responses of fire emissions to LULCC and  
1290 thus different long-term changes of fire emissions among model simulations, given  
1291 that many parameters and functions in global fire models are PFT-dependent. LUH2  
1292 used in LUMIP and ongoing CMIP6 provide information of forest/non-forest  
1293 coverage changes (Lawrence et al., 2016), which can reduce the misinterpretation of  
1294 the land use data in models and thus the inter-model spread of fire emission changes.  
1295 As discussed above, most FireMIP models do not consider the human  
1296 suppression of fire spread, decreased fuel continuity from expanding croplands and  
1297 pastures, human deforestation and degradation fires, and crop fires. Therefore, these

1298 models, and hence the CMIP6 estimates that are mainly based on them, may have  
1299 some uncertainties in estimating historical fire emissions and long-term trends. This  
1300 may further affect the estimates of the radiative forcing of fire emissions and the  
1301 historical response of trace gas and aerosol concentrations, temperature, precipitation,  
1302 and energy, water, and biogeochemical cycles to fire emissions based on  
1303 Earth/climate system models that include these fire models or are driven by such fire  
1304 emissions. It may also influence future projections of climate and Earth system  
1305 responses to various population density and land use scenarios.

1306

1307 *Author contribution.* FL contributed to the processing and analyses of the fire  
1308 emission dataset. SS and AA designed the FireMIP experiments and LF, SH, GL, CY,  
1309 DB, SM, MF, JM, and TH performed FireMIP simulations. MA compiled the EF  
1310 table. JK, AD, CI, Gv, CW provided satellite-based and CMIP estimates of fire  
1311 emissions. FL prepared the first draft of manuscript, and revised it with contributions  
1312 from ~~a~~MVM and other co-authors.

1313

1314 *Acknowledgements.* This study is co-supported by the National Key R&D Program of  
1315 China (2017YFA0604302 and 2017YFA0604804), National Natural Science  
1316 Foundation of China (41475099 and 41875137), and CAS Key Research Program of  
1317 Frontier Sciences (QYZDY-SSW-DQC002). MVM is supported by the US Joint Fire  
1318 Science Program (13-1-01-4) and the UK Leverhulme Trust through a Leverhulme  
1319 Research Centre Award (RC-2015-029). AA acknowledges support from the

1320 Helmholtz Association, its ATMO programme and the Impulse and Networking fund  
1321 which funded initial FireMIP activities. AA and SH acknowledge also the EU FP7  
1322 project BACCHUS (603445). GL is funded by the German Research Foundation  
1323 (338130981). BIM is supported by NSF (BCS-1436496). CI is supported by NASA  
1324 (NNH12ZDA001N-IDS). We are grateful to ~~Stéphane Mangeon for providing data of~~  
1325 ~~JULES-INFERNO simulations,~~ and R. J. Yokelson, Z.-D. Lin, [S. Levis](#), S. Kloster, M.  
1326 van Marle, B. Bond-Lamberty, and J. R. Marlon, and [X. Yue](#) for helpful discussions.  
1327 [We also thank two anonymous reviewers for their valuable comments and suggestions,](#)  
1328 [and Editor Qiang Zhang for handling this paper.](#)

1329

1330 *Competing interests.* The authors declare that they have no conflict of interest.

1331

## 1332 **References**

1333 Akagi, S. K., Yokelson, R. J., Wiedinmyer, C., Alvarado, M. J., Reid, J. S., Karl, T.,  
1334 Crouse, J. D., and Wennberg, P. O.: Emission factors for open and domestic  
1335 biomass burning for use in atmospheric models, *Atmos. Chem. Phys.*, 11,  
1336 4039–4072, <https://doi.org/10.5194/acp-11-4039-2011>, 2011.

1337 Andela, N., et al.: A human-driven decline in global burned area, *Science*, 356,  
1338 1356–1362, 2017.

1339 [Andela, N., Morton, D. C., Giglio, L., Paugam, R., Chen, Y., Hantson, S., van der](#)  
1340 [Werf, G. R., and Randerson, J. T.: The Global Fire Atlas of individual fire size,](#)  
1341 [duration, speed and direction, \*Earth Syst. Sci. Data\*, 11, 529–552,](#)  
1342 <https://doi.org/10.5194/essd-11-529-2019>, 2019.

1343 ~~Andela, N., Morton, D. C., Giglio, L., Paugam, R., Chen, Y., Hanson, S., van der~~  
1344 ~~Werf, G. R., and Randerson, J. T.: The Global Fire Atlas of individual fire size,~~  
1345 ~~duration, speed, and direction, Earth Syst. Sci. Data Dis.,~~  
1346 ~~<https://doi.org/10.5194/essd-2018-89>, in review, 2018.~~

1347 Andreae, M. O.: Emission of trace gases and aerosols from biomass burning – an  
1348 updated assessment, Atmos. Chem. Phys., 19, 8523–8546,  
1349 <https://doi.org/10.5194/acp-19-8523-2019>, 2019.

1350 Andreae, M. O. and Merlet, P.: Emission of trace gases and aerosols from biomass  
1351 burning, Global Biogeochem. Cy., 15, 955–966, 2001.

1352 Andreae, M. O. and Rosenfeld, D.: Aerosol–cloud– precipitation interactions, Part 1,  
1353 The nature and sources of cloud-active aerosols, Earth-Sci. Rev., 89, 13–41,  
1354 doi:10.1016/j.earscirev.2008.03.001, 2008.

1355 Archibald, S.: Managing the human component of fire regimes: lessons from  
1356 Africa, Philos. T. R. Soc. B., 371, 20150346, 2016.

1357 Arora, V. K. and Boer, G.: Fire as an interactive component of dynamic vegetation  
1358 models, J. Geophys. Res., 110, 2005.

1359 Bachelet, K. Ferschweiler, T. J. Sheehan, B. M. Sleeter, and Z. Zhu: Projected carbon  
1360 stocks in the conterminous USA with land use and variable fire regimes, Glob.  
1361 Change Biol., 21, 4548–4560, 2015.

1362 Best, M. J., et al.: The Joint UK Land Environment Simulator (JULES), model  
1363 description – Part 1: Energy and water fluxes, Geosci. Model Dev., 4, 677–699,  
1364 doi:10.5194/gmd-4-677-2011, <http://www.geosci-model-dev.net/4/677/2011/>,

1365 2011.

1366 Bistinas, S. P. Harrison, I. C. Prentice, and J. M. C. Pereira: Causal relationships  
1367 versus emergent patterns in the global controls of fire frequency, *Biogeosciences*,  
1368 11, 5087–5101, 2014.

1369 Bond-Lamberty, B., Peckham, S.D., Ahl, D.E., and Gower, S.T.: The dominance of  
1370 fire in determining carbon balance of the central Canadian boreal forest, *Nature*,  
1371 450, 89–92, 2007.

1372 Bowman, D. M. J. S., et al.: Fire in the Earth system, *Science*, 324, 481–484, 2009.

1373 Brovkin, V., et al.: Effect of anthropogenic land-use and land-cover changes on  
1374 climate and land carbon storage in CMIP5 projections for the twenty-first century,  
1375 *J. Climate*, 26, 6859–6881, doi:10.1175/JCLI-D-12-00623.1,  
1376 <http://journals.ametsoc.org/doi/abs/10.1175/JCLI-D-12-00623.1>, 2013.

1377 Chen, Y., Randerson, J., van der Werf, G., Morton, D., Mu, M., and Kasibhatla, P.:  
1378 Nitrogen deposition in tropical forests from savanna and deforestation fires, *Glob.*  
1379 *Change Biol.*, 16, 2024–2038, 2010.

1380 Ciais, P., C., et al.: Carbon and Other Biogeochemical Cycles, In: *Climate Change*  
1381 *2013: The Physical Science Basis. Contribution of Working Group I to the Fifth*  
1382 *Assessment Report of the Intergovernmental Panel on Climate Change*, edited by:  
1383 Stocker, T.F., Qin, D., Plattner, G.-K., Tignor, M., Allen, S.K., Boschung, J.,  
1384 Nauels, A., Xia, Y., Bex, V., and Midgley, P. M., Cambridge University Press,  
1385 Cambridge, United Kingdom and New York, NY, USA, 467–544, 2013.

1386 Clark, D. B. et al.: The Joint UK Land Environment Simulator (JULES), model

1387 description Part 2: Carbon fluxes and vegetation dynamics, *Geosci. Model Dev.*, 4,  
1388 701–722, doi:10.5194/gmd-4-701-2011,  
1389 <http://www.geosci-model-dev.net/4/701/2011/>, 2011.

1390 [Conedera, M., Tinner, W., Neff, C., Meurer, M., Dickens, A. F., and Krebs, P.:  
1391 Reconstructing past fire regimes: methods, applications, and relevance to fire  
1392 management and conservation, \*Quat. Sci. Rev.\*, 28, 555–576,  
1393 doi:10.1016/j.quascirev.2008.11.005, 2009.](#)

1394 Darmenov, A. S., and da Silva, A.: The Quick Fire Emissions Dataset (QFED):  
1395 Documentation of versions 2.1, 2.2 and 2.4, In: Technical Report Series on  
1396 Global Modeling and Data Assimilation, edited by Koster, R. D., NASA  
1397 Goddard Space Flight Center; Greenbelt, MD, USA, pp. 212, 2015.

1398 ~~[Duncan, B. N., Martin, R. V., Staudt, A. C., Yevich, R., and Logan, J. A.: Interannual  
1399 and seasonal variability of biomass burning emissions constrained by satellite  
1400 observations, \*J. Geophys. Res. Atmos.\*, 108, 4100, doi:10.1029/2002JD002378,  
1401 2003.](#)~~ [Falk, D. A., Heyerdahl, E. K., Brown, P. M., Farris, C., Fulé, P. Z.,  
1402 McKenzie, D., Swetnam, T. W., Taylor, A. H., and Van Horne, M. L.:  
1403 Multi-scale controls of historical forest-fire regimes: new insights from fire-scar  
1404 networks, \*Front. Ecol. Environ.\*, 9, 446–454, 2011.](#)

1405 Ferretti, D. F., et al. : Unexpected changes to the global methane budget over the past  
1406 2000 years, *Science*, 309, 1714–1717, <https://doi.org/10.1126/science.1115193>,  
1407 2005.

1408 Field, R. D., van der Werf, G. R., and Shen, S. S. P.: Human amplification of  
1409 drought-induced biomass burning in Indonesia since 1960, *Nat. Geosci.*, 2,  
1410 185–188, <https://doi.org/10.1038/ngeo443>, 2009.

1411 [Fisher, J. A., et al.: Source attribution and interannual variability of Arctic pollution in](#)  
1412 [spring constrained by aircraft \(ARCTAS, ARCPAC\) and satellite \(AIRS\)](#)  
1413 [observations of carbon monoxide, \*Atmos. Chem. Phys.\*, 10, 977–996,](#)  
1414 <https://doi.org/10.5194/acp-10-977-2010>, 2010.

1415 Grandey, B. S., Lee, H.-H., and Wang, C.: Radiative effects of interannually varying  
1416 vs. interannually invariant aerosol emissions from fires, *Atmos. Chem. Phys.*, 16,  
1417 14495–14513, <https://doi.org/10.5194/acp-16-14495-2016>, 2016.

1418 Hamilton, D. S., et al.: Reassessment of pre-industrial fire emissions strongly affects  
1419 anthropogenic aerosol forcing, *Nat. Commun.*, 9, 3182, doi:  
1420 10.1038/s41467-018-05592-9, 2018.

1421 Hantson, S., Pueyo, S., and Chuvieco, E.: Global fire size distribution is driven by  
1422 human impact and climate, *Global Ecol. Biogeogr.*, 24, 77–86, 2015.

1423 Hantson, S., et al.: The status and challenge of global fire modelling, *Biogeosciences*,  
1424 13, 3359–3375, doi:10.5194/bg-13-3359-2016, 2016.

1425 Heymann, J., Reuter, M., Buchwitz, M., Schneising, O., Bovensmann, H., Burrows, J.  
1426 P., Massart, S., Kaiser, J. W., and Crisp, D.: CO<sub>2</sub> emission of Indonesian fires in  
1427 2015 estimated from satellite-derived atmospheric CO<sub>2</sub> concentrations, *Geophys.*  
1428 *Res. Lett.*, 44, 1537–1544, 2017.

1429 Hurtt, G. C., et al.: Harmonization of land-use scenarios for the period 1500–2100:

1430 600 years of global gridded annual land-use transitions, wood harvest, and  
1431 resulting secondary lands, *Climatic Change*, 109, 117–161,  
1432 doi:10.1007/s10584-011-0153-2, 2011.

1433 Ichoku, C. and Ellison, L.: Global top-down smoke-aerosol emissions estimation  
1434 using satellite fire radiative power measurements, *Atmos. Chem. Phys.*, 14,  
1435 6643–6667, <https://doi.org/10.5194/acp-14-6643-2014>, 2014.

1436 Jiang, Y., Lu, Z., Liu, X. Qian, Y., Zhang, K., Wang, Y., and Yang, X.: Impacts of  
1437 global wildfire aerosols on direct radiative, cloud and surface-albedo forcings  
1438 simulated with CAM5, *Atmos. Chem. Phys.*, 16, 14805–14824, 2016

1439 Johnston, F. H., et al.: Estimated global mortality attributable to smoke from  
1440 landscape fires, *Environ. Health Persp.*, 120, 695–701.  
1441 <https://doi.org/10.1289/ehp.1104422>, 2012.

1442 Kaiser, J. W., Heil, A., Andreae, M. O., Benedetti, A., Chubarova, N., Jones, L.,  
1443 Morcrette, J.-J., Razinger, M., Schultz, M. G., Suttie, M., and van der Werf, G. R.:  
1444 Biomass burning emissions estimated with a global fire assimilation system based  
1445 on observed fire radiative power, *Biogeosciences*, 9, 527–554,  
1446 <https://doi.org/10.5194/bg-9-527-2012>, 2012.

1447 Keenan, T. F., Hollinger, D. Y., Bohrer, G., Dragoni, D., Munger, J. W., Schmid, H.  
1448 P., and Richardson, A. D.: Increase in forest water-use efficiency as atmospheric  
1449 carbon dioxide concentrations rise, *Nature*, 499, 324–327, 2013.

1450 Klein Goldewijk, K., Beusen, A., and Janssen, P.: Long-term dynamic modeling of  
1451 global population and built-up area in a spatially explicit way: HYDE 3.1,  
1452 Holocene, 20, 565–573, <https://doi.org/10.1177/0959683609356587>, 2010.

1453 Kloster, S., and Lasslop, G.: Historical and future fire occurrence (1850 to 2100)  
1454 simulated in CMIP5 Earth System Models, Global Planet. Change, 58–69, 2017.

1455 Kloster, S., Mahowald, N. M., Randerson, J. T., Thornton, P. E., Hoffman, F. M.,  
1456 Levis, S., Lawrence, D. M.: Fire dynamics during the 20th century simulated by  
1457 the Community Land Model. Biogeosciences, 7(6), 1877–1902.  
1458 <https://doi.org/10.5194/bg-7-1877-2010>, 2010.

1459 Knorr, W., Dentener, F., Lamarque, J.-F., Jiang, L., and Arneth, A.: Wildfire air  
1460 pollution hazard during the 21st century, Atmos. Chem. Phys., 17, 9223–9236,  
1461 <https://doi.org/10.5194/acp-17-9223-2017>, 2017.

1462 Knorr, W., Jiang, L., and Arneth, A.: Climate, CO<sub>2</sub> and human population impacts on  
1463 global wildfire emissions, Biogeosciences, 13, 267–282,  
1464 <https://doi.org/10.5194/bg-13-267-2016>, 2016.

1465 Kondo, M., et al.: Land use change and El Niño-Southern Oscillation drive decadal  
1466 carbon balance shifts in Southeast Asia, Nat. Commun., 9, 1154, doi:  
1467 [10.1038/s41467-018-03374-x](https://doi.org/10.1038/s41467-018-03374-x), 2018.

1468 [Konovalov, I. B., Lvova, D. A., Beekmann, M., Jethva, H., Mikhailov, E. F., Paris,](#)  
1469 [J.-D., Belan, B. D., Kozlov, V. S., Ciais, P., and Andreae, M. O.: Estimation of](#)  
1470 [black carbon emissions from Siberian fires using satellite observations of](#)

1471 [absorption and extinction optical depths, Atmos. Chem. Phys., 18, 14889–14924,](#)  
1472 [https://doi.org/10.5194/acp-18-14889-2018, 2018.](https://doi.org/10.5194/acp-18-14889-2018)

1473 Konovalov, I. B., Berezin, E. V., Ciais, P., Broquet, G., Beekmann, M., Hadji- Lazaro,  
1474 J., Clerbaux, C., Andreae, M. O., Kaiser, J. W., and Schulze, E.: Constraining  
1475 CO<sub>2</sub> emissions from open biomass burning by satellite observations of co-emitted  
1476 species: a method and its application to wildfires in Siberia, Atmos. Chem. Phys.,  
1477 14, 10383–10410, 2014.

1478 [Korontzi, S., McCarty, J., Loboda, T., Kumar, S., and Justice, C.: Global distribution](#)  
1479 [of agricultural fire in croplands from 3 years of Moderate Resolution Imaging](#)  
1480 [Spectroradiometer \(MODIS\) data, Global Biogeochem. Cy., 20, GB2021,](#)  
1481 [doi:10.1029/2005GB002529, 5 2006.](https://doi.org/10.1029/2005GB002529)

1482 Krinner, G., Viovy, N., de Noblet-Ducoudré, N., Ogée, J., Polcher, J., Friedlingstein,  
1483 P., Ciais, P., Sitch, S., and Prentice, I. C.: A dynamic global vegetation model for  
1484 studies of the coupled atmosphere-biosphere system, Global Biogeochem. Cy., 19,  
1485 1–33, <https://doi.org/10.1029/2003GB002199>, 2005.

1486 Krol, M., Peters, W., Hooghiemstra, P., George, M., Clerbaux, C., Hurtmans, D.,  
1487 McInerney, D., Sedano, F., Bergamaschi, P., El Hajj, M., Kaiser, J. W., Fisher, D.,  
1488 Yershov, V., and Muller, J.-P.: How much CO was emitted by the 2010 fires  
1489 around Moscow? Atmos. Chem. Phys., 13(9):4737–4747, 2013.

1490 Lamarque, J.-F., et al.: Historical (1850–2000) gridded anthropogenic and biomass  
1491 burning emissions of reactive gases and aerosols: methodology and application,

1492 Atmos. Chem. Phys., 10, 7017-7039, <https://doi.org/10.5194/acp-10-7017-2010>,  
1493 2010.

1494 Lasslop, G., Thonicke, K., and Kloster, S.: SPITFIRE within the MPI Earth system  
1495 model: Model development and evaluation, *J. Adv. Model Earth Sy.*, 6, 740–755,  
1496 <https://doi.org/10.1002/2013MS000284>, 2014.

1497 [Lawrence, D. M., et al.: The Land Use Model Intercomparison Project \(LUMIP\)](#)  
1498 [contribution to CMIP6: rationale and experimental design, \*Geosci. Model Dev.\*, 9,](#)  
1499 [2973–2998, <https://doi.org/10.5194/gmd-9-2973-2016>, 2016.](#)

1500 Legrand, M., et al.: Boreal fire records in Northern Hemisphere ice cores: a review,  
1501 *Clim. Past*, 12, 2033-2059, <https://doi.org/10.5194/cp-12-2033-2016>, 2016.

1502 Lehsten, V., Tansey, K., Balzter, H., Thonicke, K., Spessa, A., Weber, U., Smith, B.,  
1503 and Arneeth, A.: Estimating carbon emissions from African wildfires,  
1504 *Biogeosciences*, 6, 349-360, <https://doi.org/10.5194/bg-6-349-2009>, 2009.

1505 Lelieveld, J., Evans, J. S., Fnais, M., Giannadaki, D., and Pozzer, A.: The con-  
1506 tribution of outdoor air pollution sources to premature mortality on a global scale,  
1507 *Nature*, 525, 367– 371, 2015.

1508 Le Page, Y., Morton, D., Bond-Lamberty, B., Pereira, J. M. C., and Hurtt, G.:  
1509 HESFIRE: A global fire model to explore the role of anthropogenic and weather  
1510 drivers, *Biogeosciences*, 12, 887–903, <https://doi.org/10.5194/bg-12-887-2015>,  
1511 2015.

1512 [Le Page, Y., Morton, D., Hartin, C., Bond-Lamberty, B., Pereira, J. M. C., Hurtt, G.,](#)  
1513 [and Asrar, G.: Synergy between land use and climate change increases future fire](#)

1514 [risk in Amazon forests, Earth Syst. Dynam., 8, 1237–1246,](#)  
1515 <https://doi.org/10.5194/esd-8-1237-2017>, 2017.

1516 Le Quéré, C., et al.: Global carbon budget 2013, Earth Syst. Sci. Data, 6, 235–263,  
1517 doi:10.5194/essd-6-235-2014, <http://www.earth-syst-sci-data.net/6/235/2014/>,  
1518 2014.

1519 Levis, S., Bonan, G. B., Vertenstein, M., and Oleson, K. W.: The Community Land  
1520 Model's dynamic global vegetation model (CLM-DGVM): Technical description  
1521 and user's guide, NCAR Tech. Note TN-459 IA, Terrestrial Sciences Section,  
1522 Boulder, Colorado, 2004.

1523 Li, F., Zeng, X.-D., Levis, S.: A process-based fire parameterization of intermediate  
1524 complexity in a Dynamic Global Vegetation Model, Biogeosciences, 9,  
1525 2761–2780, 2012.

1526 Li, F., Levis, S., and Ward, D. S.: Quantifying the role of fire in the Earth system—Part  
1527 1: Improved global fire modeling in the Community Earth System Model  
1528 (CESM1), Biogeosciences, 10, 2293–2314, 2013.

1529 Li, F., and Lawrence, D. M.: Role of fire in the global land water budget during the  
1530 20th century through changing ecosystems, J. Clim., 30, 1893–908, 2017.

1531 Li, F., Lawrence, D.M., Bond-Lamberty, B.: Human impacts on 20th century fire  
1532 dynamics and implications for global carbon and water trajectories, Glob. Planet.  
1533 Change, 162, 18–27, 2018.

1534 Lindeskog, M., Arneth, A., Bondeau, A., Waha, K., Seaquist, J., Olin, S., and Smith,  
1535 B.: Implications of accounting for land use in simulations of ecosystem carbon

1536 cycling in Africa, *Earth Syst. Dynam.*, 4, 385–407, doi:10.5194/esd-4-385-2013,  
1537 2013.

1538 Magi, B.I., Rabin, S., Shevliakova, E., Pacala, S.: Separating agricultural and  
1539 non-agricultural fire seasonality at regional scales, *Biogeosciences*, 9,  
1540 3003–3012, 2012.

1541 Mahowald, N., et al.: Global distribution of atmospheric phosphorus sources,  
1542 concentrations and deposition rates, and anthropogenic impacts, *Global*  
1543 *Biogeochem. Cy.*, 22, GB4026, doi: 10.1029/2008GB003240, 2008.

1544 Mangeon, S., Voulgarakis, A., Gilham, R., Harper, A., Sitch, S., and Folberth, G.:  
1545 INFERNO: a fire and emissions scheme for the UK Met Office’s Unified Model,  
1546 *Geosci. Model Dev.*, 9, 2685–2700, doi:10.5194/gmd-9-2685-2016,  
1547 <http://www.geosci-model-dev.net/9/2685/2016/>, 2016.

1548 Mao, J. F., Wang, B., and Dai, Y. J.: Sensitivity of the carbon storage of potential  
1549 vegetation to historical climate variability and CO<sub>2</sub> in continental China, *Adv.*  
1550 *Atmos. Sci.*, 26, 87–100, 2009.

1551 Marlier, M. E., DeFries, R. S., Voulgarakis, A., Kinney, P. L., Randerson, J. T.,  
1552 Shindell, D. T., Chen, Y., and Faluvegi, G.: El Niño and health risks from  
1553 landscape fire emissions in southeast Asia, *Nat. Clim. Change*, 3, 131–136, 2013.

1554 Marlon, J. R., et al.: Climate and human influences on global biomass  
1555 burning over the past two millennia, *Nat. Geosci.*, 1, 697–702,  
1556 <https://doi.org/10.1038/ngeo313>, 2008.

1557 Marlon, J. R., et al.: Reconstructions of biomass burning from sediment–charcoal

1558 records to improve data–model comparisons, *Biogeosciences*, 13, 3225–3244,  
1559 <https://doi.org/10.5194/bg-13-3225-2016>, 2016.

1560 McConnell, J. R., Edwards, R., Kok, G. L., Flanner, M. G., Zender, C. S., Saltzman, E.  
1561 S., Banta, J. R., Pasteris, D. R., Carter, M. M., and Kahl, J. D. W.: 20th-century  
1562 industrial black carbon emissions altered arctic climate forcing, *Science*, 317,  
1563 1381–1384, doi:10.1126/science.1144856, 2007.

1564 ~~[McKendry, I. G., Christen, A., Lee, S.-C., Ferrara, M., Strawbridge, K. B., O'Neill, N.,](#)~~  
1565 ~~[and Black, A.: Impacts of an intense wildfire smoke episode on surface radiation,](#)~~  
1566 ~~[energy and carbon fluxes in southwestern British Columbia, Canada, \*Atmos.\*](#)~~  
1567 ~~[Chem. Phys.](#), 19, 835–846, <https://doi.org/10.5194/acp-19-835-2019>, 2019.~~

1568 ~~[McMeeking, G. R., et al.: Emissions of trace gases and aerosols during the open-](#)~~  
1569 ~~[combustion of biomass in the laboratory, \*J. Geophys. Res.\*, 114, D19210,](#)~~  
1570 ~~[doi:10.1029/2009JD011836, 2009.](#)~~

1571 Melton, J. R., and Arora, V. K.: Competition between plant functional types in the  
1572 Canadian Terrestrial Ecosystem Model (CTEM) v. 2.0, *Geosci. Model Dev.*, 9,  
1573 323–361, doi:10.5194/gmd-9-323-2016, 2016.

1574 Mieville, A., Granier, C., Lioussé, C., Guillaume, B., Mouillot, F., Lamarque, J.-F.,  
1575 Grégoire, J.-M., and Pétron, G.: Emissions of gases and particles from biomass  
1576 burning during the 20th century using satellite data and an historical  
1577 reconstruction, *Atmos. Environ.*, 44, 1469–1477,  
1578 <https://doi.org/10.1016/j.atmosenv.2010.01.011>, 2010.

1579 Mouillot, F. and Field, C. B.: Fire history and the global carbon budget: a 1°×1°fire  
1580 history reconstruction for the 20th century, *Glob. Change Biol.*, 11, 398–420,  
1581 <https://doi.org/10.1111/j.1365-2486.2005.00920.x>, 2005.

1582 Nemani, R.R., and Running, S.W.: Implementation of a hierarchical global vegetation  
1583 classification in ecosystem function models, *J. Veg. Sci.*, 7, 337-346, 1996.

1584 Oleson, K., et al.: Technical Description of version 4.5 of the Community Land  
1585 Model (CLM), Tech. Rep. NCAR/TN-503+STR NCAR, Boulder, CO, USA,  
1586 pp.434, 2013.

1587 Parisien, M., Miller, C., Parks, S.A., DeLancey, E.R., Robinne, F., and Flannigan, M.  
1588 D.: The spatially varying influence of humans on fire probability in North  
1589 America, *Environ. Res. Lett.*, 11:075005, 2016.

1590 Pechony, O., and Shindell, D.T.: Driving forces of global wildfires over the past  
1591 millennium and the forthcoming century, *P. Natl. Acad. Sci. USA*, 107,  
1592 19167–19170, 2010.

1593 Pfeiffer, M., Spessa, A., and Kaplan, J. O.: A model for global biomass burning in  
1594 preindustrial time: LPJ-LMfire (v1.0), *Geosci. Model Dev.*, 6, 643–685,  
1595 [doi:10.5194/gmd-6-643-2013](https://doi.org/10.5194/gmd-6-643-2013), 2013.

1596 Rabin, S. S., et al.: The Fire Modeling Intercomparison Project (FireMIP),  
1597 phase 1: experimental and analytical protocols with detailed model descriptions.  
1598 *Geosci. Model Dev.*, 10, 1175–1197, 2017.

1599 Rabin, S. S., Ward, D. S., Malyshev, S. L., Magi, B. I., Shevliakova, E., and Pacala, S.  
1600 W.: A fire model with distinct crop, pasture, and non-agricultural burning: use of

1601 new data and a model-fitting algorithm for FINAL.1, *Geosci. Model Dev.*, 11,  
1602 815–842, <https://doi.org/10.5194/gmd-11-815-2018>, 2018.

1603 [Reddington, C. L., Morgan, W. T., Darbyshire, E., Brito, J., Coe, H., Artaxo, P., Scott,](#)  
1604 [C. E., Marsham, J., and Spracklen, D. V.: Biomass burning aerosol over the](#)  
1605 [Amazon: analysis of aircraft, surface and satellite observations using a global](#)  
1606 [aerosol model, \*Atmos. Chem. Phys.\*, 19, 9125–9152,](#)  
1607 <https://doi.org/10.5194/acp-19-9125-2019>, 2019.

1608 [Randerson, J. T., Chen, Y., van der Werf, G. R., Rogers, B. M., and Morton, D. C.:](#)  
1609 [Global burned area and biomass burning emissions from small fires, \*J. Geophys.\*](#)  
1610 [Res., 117, G04012, <https://doi.org/10.1029/2012JG002128>, 2012.](#)

1611

1612 Rothermel, R. C.: A mathematical model for predicting fire spread in wildland fuels,  
1613 Res. Pap. INT-115, US Department of Agriculture, Ogden, UT, USA, pp. 40,  
1614 1972.

1615 Schultz, M. G., Heil, A., Hoelzemann, J. J., Spessa, A., Thonicke, K., Goldammer, J.  
1616 G., Held, A. C., Pereira, J. M. C., and van het Bolscher, M.: Global wildland fire  
1617 emissions from 1960 to 2000, *Global Biogeochem. Cy.*, 22, GB2002,  
1618 <https://doi.org/10.1029/2007GB003031>, 2008.

1619 Scott, A. C., and Glasspool, I. J.: The diversification of Palaeozoic fire systems and  
1620 fluctuations in atmospheric oxygen concentration, *Proc. Natl. Acad. Sci. U.S.A.*,  
1621 103, 10861–10865, doi:10.1073/pnas.0604090103, 2006.

1622 Sheehan, T., Bachelet, D., and Ferschweiler, K.: Projected major fire and vegetation

1623 changes in the Pacific Northwest of the conterminous United States under  
1624 selected CMIP5 climate futures, *Ecol. Model.*, 317, 16–29,  
1625 doi:10.1016/j.ecolmodel.2015.08.023, 2015.

1626 Smith, B., Wårlind, D., Arneth, A., Hickler, T., Leadley, P., Siltberg, J., and Zaehle,  
1627 S.: Implications of incorporating N cycling and N limitations on primary  
1628 production in an individual-based dynamic vegetation model, *Biogeosciences*, 11,  
1629 2027–2054, doi:10.5194/bg-11-2027-2014, 2014.

1630 Stockwell, C. E., et al.: Nepal Ambient Monitoring and Source Testing Experiment  
1631 (NAMaSTE): emissions of trace gases and light-absorbing carbon from wood and  
1632 dung cooking fires, garbage and crop residue burning, brick kilns, and other  
1633 sources, *Atmos. Chem. Phys.*, 16, 11043–11081, 2016.

1634 Thonicke, K., Spessa, A., Prentice, I. C., Harrison, S. P., Dong, L., and  
1635 Carmona-Moreno, C.: The influence of vegetation, fire spread and fire behaviour  
1636 on biomass burning and trace gas emissions: Results from a process-based model,  
1637 *Biogeosciences*, 7, 1991–2011, 2010.

1638 Thonicke, K., Venevsky, S., Sitch, S., and Cramer, W.: The role of fire disturbance  
1639 for global vegetation dynamics: Coupling fire into a Dynamic Global Vegetation  
1640 Model, *Global Ecol. Biogeogr.*, 10, 661–677, 2001.

1641 Thornhill, G. D., Ryder, C. L., Highwood, E. J., Shaffrey, L. C., and Johnson, B. T.:  
1642 The effect of South American biomass burning aerosol emissions on the regional  
1643 climate, *Atmos. Chem. Phys.*, 18, 5321–5342,  
1644 <https://doi.org/10.5194/acp-18-5321-2018>, 2018.

1645 Tian, H., et al.: The terrestrial biosphere as a net source of greenhouse gases to the  
1646 atmosphere, *Nature*, 531, 225–228, 2016.

1647 Tosca, M. G., Randerson, J. T., and Zender, C. S.: Global impact of smoke aerosols  
1648 from landscape fires on climate and the Hadley circulation, *Atmos. Chem. Phys.*,  
1649 13, 5227–5241, <https://doi.org/10.5194/acp-13-5227-2013>, 2013.

1650 [Teckentrup, L., Harrison, S. P., Hantson, S., Heil, A., Melton, J. R., Forrest, M., Li, F.,](#)  
1651 [Yue, C., Arneeth, A., Hickler, T., Sitch, S., and Lasslop, G.: Sensitivity of](#)  
1652 [simulated historical burned area to environmental and anthropogenic controls: A](#)  
1653 [comparison of seven fire models, \*Biogeosciences Discuss.\*,](#)  
1654 <https://doi.org/10.5194/bg-2019-42>, 2019.

1655 Val Martin, M., Heald, C.L., Lamarque, J.F., Tilmes, S., Emmons, L.K., Schichtel,  
1656 B.A.: How emissions, climate, and land use change will impact mid-century air  
1657 quality over the United States: a focus on effects at national parks, *Atmos. Chem.*  
1658 *Phys.* 15, 2805-2823, 2015.

1659 van der Werf, G. R., Peters, W., van Leeuwen, T. T., and Giglio, L: What could have  
1660 caused pre-industrial biomass burning emissions to exceed current rates?, *Clim.*  
1661 *Past*, 9, 289–306, <http://www.clim-past.net/9/289/2013/>, 2013.

1662 [van der Werf, G. R., Randerson, J. T., Giglio, L., Collatz, G. J., Kasibhatla, P. S., and](#)  
1663 [Arellano Jr., A. F.: Interannual variability in global biomass burning emissions](#)  
1664 [from 1997 to 2004, \*Atmos. Chem. Phys.\*, 6, 3423-3441,](#)  
1665 <https://doi.org/10.5194/acp-6-3423-2006>, 2006.

1666 van der Werf, G. R., Randerson, J. T., Giglio, L., Collatz, G. J., Mu, M., Kasibhatla, P.  
1667 S., Morton, D. C., DeFries, R. S., Jin, Y., and van Leeuwen, T. T.: Global fire  
1668 emissions and the contribution of deforestation, savanna, forest, agricultural,  
1669 and peat fires (1997–2009), *Atmos. Chem. Phys.*, 10, 11707–11735,  
1670 <https://doi.org/10.5194/acp-10-11707-2010>, 2010.

1671 van der Werf, G. R., et al.: Global fire emissions estimates during  
1672 1997–2016, *Earth Syst. Sci. Data.*, 9, 679–720, 2017.

1673 van Marle, M. J. E., Field, R. D., van der Werf, G. R., Estrada de Wagt, I. A.,  
1674 Houghton, R. A., Rizzo, L. V., Artaxo, P., and Tsigaridis, K.: Fire and  
1675 deforestation dynamics in Amazonia (1973–2014), *Global Biogeochem. Cy.*, 31,  
1676 24–38, <https://doi.org/10.1002/2016GB005445>, 2017a.

1677 van Marle, M. J. E., et al., Historic global biomass burning emissions based on  
1678 merging satellite observations with proxies and fire models (1750 - 2015), *Geosci.*  
1679 *Model Dev.*, 10, 3329-3357, doi:10.5194/gmd-2017-32, 2017b.

1680 Wang, Z., et al.: The isotopic record of Northern Hemisphere atmospheric carbon  
1681 monoxide since 1950: implications for the CO budget, *Atmos. Chem. Phys.*, 12,  
1682 4365–4377, <https://doi.org/10.5194/acp-12-4365-2012>, 2012.

1683 Ward, D. S., Kloster, S., Mahowald, N. M., Rogers, B.M., Randerson, J. T., Hess, P.  
1684 G.: The changing radiative forcing of fires: Global model estimates for past,  
1685 present and future, *Atmos. Chem. Phys.* 12, 10857–10886, 2012.

1686 Ward, D. S., Shevliakova, E., Malyshev, S., Rabin, S.: Trends and variability  
1687 of global fire emissions due to historical anthropogenic activities. *Global*

1688 Biogeochem. Cy.,32, 122–142, <https://doi.org/10.1002/2017GB005787>,  
1689 2018.

1690 Wei, Y., et al.: The North American Carbon Program Multi-scale Synthesis and  
1691 Terrestrial Model Intercomparison Project – Part 2: Environmental driver data,  
1692 Geoscientific Model Development, 7, 2875–2893, doi:10.5194/gmd-7-2875-2014,  
1693 2014.

1694 Wiedinmyer, C., Akagi, S. K., Yokelson, R. J., Emmons, L. K., Al-Saadi, J. A.,  
1695 Orlando, J. J., and Soja, A. J. : The Fire INventory from NCAR (FINN): A high  
1696 resolution global model to estimate the emissions from open burning, Geosci.  
1697 Model Dev., 4, 625–641, <https://doi.org/10.5194/gmd-4-625-2011>, 2011

1698 Wu, Y., Han, Y., Voulgarakis, A., Wang, T., Li, M., Wang, Y., Xie, M., Zhuang, B.,  
1699 and Li, S.: An agricultural biomass burning episode in eastern China: Transport,  
1700 optical properties, and impacts on regional air quality, J. Geophys. Res.-Atmos.,  
1701 122, 2304–2324, doi:10.1002/2016JD025319, 2017.

1702 Yang, J., Tian, H., Tao, B., Ren, W., Kush, J., Liu, Y., and Wang, Y.: Spatial and  
1703 temporal patterns of global burned area in response to anthropogenic and  
1704 environmental factors: Reconstructing global fire history for the 20th and early  
1705 21st centuries, J. Geophys. Res, -Biogeo., 119, 249–263.  
1706 <https://doi.org/10.1002/2013JG002532>, 2014.

1707 Yokelson, R. J., et al.: Coupling field and laboratory measurements to estimate the  
1708 emission factors of identified and unidentified trace gases for prescribed fires,  
1709 Atmos. Chem. Phys., 13, 89–116, doi:10.5194/acp-13-89-2013, 2013.

1710 Yue, C., Ciais, P., Cadule, P., Thonicke, K., and van Leeuwen, T. T.: Modelling the  
1711 role of fires in the terrestrial carbon balance by incorporating SPITFIRE into the  
1712 global vegetation model ORCHIDEE– Part 2: Carbon emissions and the role of  
1713 fires in the global carbon balance, *Geosci. Model Dev.*, 8, 1321–1338,  
1714 <https://doi.org/10.5194/gmd-8-1321-2015>, 2015.

1715 Yue, C., et al.: Modelling the role of fires in the terrestrial carbon balance by  
1716 incorporating SPITFIRE into the global vegetation model ORCHIDEE – Part 1:  
1717 simulating historical global burned area and fire regimes, *Geosci. Model Dev.*, 7,  
1718 2747–2767, <https://doi.org/10.5194/gmd-7-2747-2014>, 2014.

1719 Yue, X., and Unger, N.: Fire air pollution reduces global terrestrial productivity,  
1720 *nature commun.*, 9, 5413, <https://doi.org/10.1038/s41467-018-07921-4>, 2018.

1721 Zennaro, P., et al.: Fire in ice: two millennia of boreal forest fire history from the  
1722 Greenland NEEM ice core, *Clim. Past*, 10, 1905–1924,  
1723 <https://doi.org/10.5194/cp-10-1905-2014>, 2014.

1724 Zhang, F., Wang, J., Ichoku, C., Hyer, E. J., Yang, Z., Ge, C., Su, S., Zhang, X.,  
1725 Kondragunta, S., Kaiser, J. W., Wiedinmyer, C., and da Silva, A.: Sensitivity of  
1726 mesoscale modeling of smoke direct radiative effect to the emission inventory: a  
1727 case study in northern sub-Saharan African region, *Environ. Res. Lett.*, 9, 075002,  
1728 [doi:10.1088/1748-9326/9/7/075002](https://doi.org/10.1088/1748-9326/9/7/075002), 2014.

1729 [Zhang, T. R., Wooster, M. J., de Jong, M. C., and Xu, W. D.: How well does the](#)  
1730 [‘Small Fire Boost’ methodology used within the GFED4.1s fire emissions](#)

1731 [database represent the timing, location and magnitude of agricultural burning?](#)  
1732 [Remote. Sens., 10, 823, doi:10.3390/rs10060823, 2018.](#)  
1733 Zhu, Z., et al: Greening of the Earth and its drivers, Nat. Clim. Change, 6, 791–795,  
1734 2016.

**Table 1.** Summary description of the Dynamic Global Vegetation Models (DGVMs)

participated in FireMIP.

<u>DGVMs</u>	<u>tem. res. of model outputs</u>	<u>spatial res. of model outputs</u>	<u>period</u>	<u>natural veg. distrib.</u>	<u>fire scheme ref.</u>	<u>DGVM ref.</u>
<u>CLM4.5 but CLM5 fire model (CLM4.5)</u>	<u>monthly</u>	<u>~1.9° (lat) ×2.5° (lon)</u>	<u>1700– 2012</u>	<u>P</u>	<u>Li et al. (2012, 2013) Li and Lawrence (2017)</u>	<u>Oleson et al. (2013)</u>
<u>CTEM</u>	<u>monthly</u>	<u>2.8125°</u>	<u>1861– 2012</u>	<u>P</u>	<u>Arora and Boer (2005) Melton and Arora (2016)</u>	<u>Melton and Arora (2016)</u>
<u>JSBACH-SPITFIRE (JSBACH)</u>	<u>monthly</u>	<u>1.875°</u>	<u>1700– 2012</u>	<u>P</u>	<u>Lasslop et al. (2014) Thonicke et al. (2010)</u>	<u>Brovkin et al. (2013)</u>
<u>JULES-INFERNO (JULES)</u>	<u>monthly</u>	<u>~1.2° (lat) ×1.9°(lon)</u>	<u>1700– 2012</u>	<u>M</u>	<u>Mangeon et al. (2016)</u>	<u>Best et al. (2011) Clark et al. (2011)</u>
<u>LPJ-GUESS-GlobFIR M (LGG)</u>	<u>annual</u>	<u>0.5°</u>	<u>1700– 2012</u>	<u>M</u>	<u>Thonicke et al. (2001)</u>	<u>Smith et al. (2014) Lindeskog et al. (2013)</u>
<u>LPJ-GUESS-SPITFIRE (LGS)</u>	<u>monthly</u>	<u>0.5°</u>	<u>1700– 2012</u>	<u>M</u>	<u>Lehsten et al. (2009) Rabin et al. (2017)</u>	<u>Smith et al. (2001) Ahlstrom et al. (2012)</u>
<u>LPJ-GUESS-SIMFIRE -BLAZE (LGSB)</u>	<u>monthly</u>	<u>0.5°</u>	<u>1700– 2012</u>	<u>M</u>	<u>Knorr et al. (2016)</u>	<u>Smith et al. (2014) Lindeskog et al. (2013) Nieradzki et al. (2017)</u>
<u>MC2</u>	<u>annual</u>	<u>0.5°</u>	<u>1901– 2008</u>	<u>M</u>	<u>Bachelet et al. (2015) Sheehan et al. (2015)</u>	<u>Bachelet et al. (2015) Sheehan et al. (2015)</u>
<u>ORCHIDEE-SPITFIRE (ORCHIDEE)</u>	<u>monthly</u>	<u>0.5°</u>	<u>1700– 2012</u>	<u>P</u>	<u>Yue et al. (2014, 2015) Thonicke et al. (2010)</u>	<u>Krinner et al. (2005)</u>

Acronym: CLM4.5 and CLM5: Community Land Model version 4.5 and 5; CTEM: Canadian Terrestrial Ecosystem Model; JSBACH: Jena Scheme for Biosphere-Atmosphere Coupling in Hamburg; SPITFIRE: Spread and InTensity fire model; JULES: Joint UK Land Environment Simulator; INFERNO: Interactive Fire And Emission Algorithm For Natural Environments; GlobFIRM: fire module Global FIRE Model; SMIFIRE: SIMple FIRE model; BLAZE: Blaze-Induced Land-Atmosphere Flux Estimator; ORCHIDEE: Organizing Carbon Hydrology In Dynamic Ecosystems; PFT: plant functional type; P: prescribed; M: modeled

**Table 2. Summary description of global fire modules in FireMIP DGVMs.**

DGVMs	<u>crop fire</u>	<u>tropical human defor. fire</u>	<u>human ignition</u>	<u>human fire suppression</u>	<u>peat fire</u>	<u>pasture</u>	<u>combust. complete. range of woody tissue</u>
<u>CLM4.5</u>	<u>yes</u>	<u>yes</u>	<u>increase with PD<sup>a</sup></u>	<u>occurrence &amp; spread area<sup>b</sup></u>	<u>yes<sup>c</sup></u>	<u>as natural grassland</u>	<u>27–35% (stem) 40% (CWD<sup>f</sup>)</u>
<u>CTEM</u>	<u>no</u>	<u>no</u>	<u>increase with PD</u>	<u>occurrence &amp; duration<sup>c</sup></u>	<u>no</u>	<u>as natural grassland</u>	<u>6% (stem) 15–18% (CWD)</u>
<u>JSBACH</u>	<u>as grass fire</u>	<u>no</u>	<u>increase with PD</u>	<u>occurrence &amp; duration<sup>c</sup></u>	<u>no</u>	<u>high fuel bulk den.</u>	<u>0–45%</u>
<u>JULES</u>	<u>no</u>	<u>no</u>	<u>increase with PD</u>	<u>occurrence<sup>c</sup></u>	<u>no</u>	<u>as natural grassland</u>	<u>0–40%</u>
<u>LGG</u>	<u>no</u>	<u>no</u>	<u>no</u>	<u>no</u>	<u>no</u>	<u>harvest</u>	<u>70–90%</u>
<u>LGS</u>	<u>no</u>	<u>no</u>	<u>increase with PD</u>	<u>occurrence<sup>c</sup></u>	<u>no</u>	<u>as natural grassland</u>	<u>0–98% (100h<sup>g</sup>) 0–80% (1000h<sup>g</sup>)</u>
<u>LGSB</u>	<u>no</u>	<u>no</u>	<u>increase with PD</u>	<u>burned area<sup>c</sup></u>	<u>no</u>	<u>harvest</u>	<u>0–50%</u>
<u>MC2</u>	<u>no</u>	<u>no</u>	<u>no</u>	<u>occurrence<sup>d</sup></u>	<u>no</u>	<u>as natural grassland</u>	<u>0–87% (100h) 0–43% (1000h)</u>
<u>ORCHIDEE</u>	<u>no</u>	<u>no</u>	<u>increase with PD</u>	<u>occurrence<sup>c</sup></u>	<u>no</u>	<u>as natural grassland</u>	<u>0–73% (100h) 0–41% (1000h)</u>

<sup>a</sup> PD: population density

<sup>b</sup> fire suppression increases with PD and GDP, different between tree PFTs and grass/shrub PFTs

<sup>c</sup> fire suppression increases with PD

<sup>d</sup> Assume no fire in grid cell when pre-calculated rate of spread, fireline intensity, and energy release component are lower than thresholds

<sup>e</sup> CLM4.5 outputs in FireMIP include biomass and litter burning due to peat fires, but don't include burning of soil organic matter

<sup>f</sup> Coarse Woody Debris

<sup>g</sup> 100-hour fuels and 1000-hour fuel classes

**Table 32.** Emission factors (g species (kg DM)<sup>-1</sup>) for land cover types (LCTs).

No.	Species	grassland /savanna	tropical forest	temperate forest	boreal forest	cropland
1	CO <sub>2</sub>	1647	1613	1566	1549	1421
2	CO	70	108	112	124	78
3	CH <sub>4</sub>	2.5	6.3	5.8	5.1	5.9
4	NMHC	5.5	7.1	14.6	5.3	5.8
5	H <sub>2</sub>	0.97	3.11	2.09	1.66	2.65
6	NO <sub>x</sub>	2.58	2.55	2.90	1.69	2.67
7	N <sub>2</sub> O	0.18	0.20	0.25	0.25	0.09
8	PM <sub>2.5</sub>	7.5	8.3	18.1	20.2	8.5
9	TPM	8.5	10.9	18.1	15.3	11.3
10	TPC	3.4	6.0	8.4	10.6	5.5
11	OC	3.1	4.5	8.9	10.1	5.0
12	BC	0.51	0.49	0.66	0.50	0.43
13	SO <sub>2</sub>	0.51	0.78	0.75	0.75	0.81
14	C <sub>2</sub> H <sub>6</sub> (ethane)	0.42	0.94	0.71	0.90	0.76
15	CH <sub>3</sub> OH (methanol)	1.48	3.15	2.13	1.53	2.63
16	C <sub>3</sub> H <sub>8</sub> (propane)	0.14	0.53	0.29	0.28	0.20
17	C <sub>2</sub> H <sub>2</sub> (acetylene)	0.34	0.43	0.35	0.27	0.32
18	C <sub>2</sub> H <sub>4</sub> (ethylene)	1.01	1.11	1.22	1.49	1.14
19	C <sub>3</sub> H <sub>6</sub> (propylene)	0.49	0.86	0.67	0.66	0.48
20	C <sub>5</sub> H <sub>8</sub> (isoprene)	0.12	0.22	0.19	0.07	0.18
21	C <sub>10</sub> H <sub>16</sub> (terpenes)	0.10	0.15	1.07	1.53	0.03
22	C <sub>7</sub> H <sub>8</sub> (toluene)	0.20	0.23	0.43	0.32	0.18
23	C <sub>6</sub> H <sub>6</sub> (benzene)	0.34	0.38	0.46	0.52	0.31
24	C <sub>8</sub> H <sub>10</sub> (xylene)	0.09	0.09	0.17	0.10	0.09
25	CH <sub>2</sub> O (formaldehyde)	1.33	2.40	2.22	1.76	1.80
26	C <sub>2</sub> H <sub>4</sub> O (acetaldehyde)	0.86	2.26	1.20	0.78	1.82
27	C <sub>3</sub> H <sub>6</sub> O (acetone)	0.47	0.63	0.70	0.61	0.61
28	C <sub>3</sub> H <sub>6</sub> O <sub>2</sub> (hydroxyacetone)	0.52	1.13	0.85	1.48	1.74
29	C <sub>6</sub> H <sub>5</sub> OH (Phenol)	0.37	0.23	0.33	2.96	0.50
30	NH <sub>3</sub> (ammonia)	0.91	1.45	1.00	2.82	1.04
31	HCN (hydrogen cyanide)	0.42	0.38	0.62	0.81	0.43
32	MEK/2-butanone	0.13	0.50	0.23	0.15	0.60
33	CH <sub>3</sub> CN (acetonitrile)	0.17	0.51	0.23	0.30	0.25

**Table 43.** Attribution of plant function types (PFTs) in FireMIP DGVMs to land cover types (LCTs) for emission factors described in Table 2.

LCT Models	Grassland /Savannas	Tropical Forest	Temperate Forest	Boreal Forest	Cropland
CLM4.5	A C3/C3/C4 G Bor BD S Tem BE/BD S	Tro BE T Tro BD T	Tem NE T Tem BE T Tem BD T	Bor NE T Bor ND T Bor BD T	Crop
CTEM	C3/C4 G	BE T <sup>a</sup> Other BD T <sup>a</sup>	NE/BE T <sup>a</sup> Other BD T <sup>a</sup>	NET <sup>a</sup> , ND T Cold BD T	C3/C4 Crop
JSBACH	C3/C4 G/P	Tro E/D T	Ex-Tro E/D T <sup>a</sup>	Ex-Tro E/D T <sup>a</sup>	Crop
JULES	C3/C4 G E/D S	Tro BE T BD T <sup>a</sup>	Tem BE T BD/NE T <sup>a</sup>	BD/NE T <sup>a</sup> NDT	
LGG <sup>b</sup>	C3/C4 G C3/C4 G in P	Tro BE/BR T Tro SI BE T	Tem NSG/BSG/BE T Tem SI SG B T	Bor NE T Bor SI NE T	R/I S/W Wheat R/I Maize
LGS	C3/C4 G	Tro BE/BR T Tro SI BE T	Tem SI&SG B T Tem B/N E T	Bor NE T Bor SI&SG NE/N T	
LGSB <sup>b</sup>	C3/C4 G C3/C4 G in P	Tro BE/BR T Tro SI BE T	Tem NSG/BSG/ BE T Tem SI SG B T	Bor NE T Bor SI NE T	R/I S/W Wheat R/I Maize
MC2	Tem C3 G/S Sub-Tro C4 G/S Tro S/G/Sava Bor M W Tem/Sub-Tro NE/B/M W Tundra Taiga-Tundra	Tro BE T Tro D W <sup>c</sup>	Maritime NE F Sub-Tro NE/BD/BE/M – F Tem NE/BD F Tem C/W M F	Bor NE F Subalpine F Cool N F	
ORCHIDEE	C3/C4 G	Tro B E/R T	Tem N/B E T Tem BD T	Bor N E/D T Bor BT T	C3/C4 Crop

Acronym: T: tree; S: shrub; W: woodland; F: forest; G: grass; P: pasture; Sava: Savanna; N: needleleaf; E: evergreen; B: broadleaf; D: deciduous; R: raingreen; SI: shaded-intolerant; SG: summer-green; M: mixed; I: irrigated; RF: rainfed; C/W: cool or warm; S/W: spring or winter, Tro: Tropical; Tem: Temperate; Bor: Boreal; Sub-Tro: subtropical; Ex-Tro: Extratropical; A: Arctic

<sup>a</sup> split tree PFTs into tropical, temperate, and boreal groups following rules of Nemani and Running (1996) that also used to make CLM land surface data by Peter et al. (2007; 2012) since CLM version 3

<sup>b</sup> LGG and LGSB did not outputs PFT-level fire carbon emissions, so land cover classified using its dominant vegetation type

<sup>c</sup> MC2 classifies tropical savannas and tropical deciduous woodland regions, and the latter mainly represents tropical deciduous forests

**Table 54.** Summary description of satellite-based products and historical

constructions merged from multiple sources.

Name	Method	Fire data sources	Peat burning	Start year	reference
GFED4	Bottom-up: fuel consumption,	MODIS, VIRS/ATSR	Y	1997	van der Werf et al. (2017)
GFED4s	burned area & active fire counts		Y	1997	
GFAS1.2	(GFED4&4s), FRP (GFAS1),	MODIS	Y	2001	Kaiser et al. (2012)
FINN1.5	active fire counts (FINN1.5), emis. factor	MODIS	N	2003	Wiedinmyer et al. (2011)
FEER1	Top-down: FRP, satellite AOD	MODIS, SEVIRI	Y	2003	Ichoku and Ellison (2014)
QFED2.5	constrained, emis. factor	MODIS	N	2001	Darmenov and da Silva (2015)
CMIP5	Merged decadal fire trace gas and aerosol emis.	GFED2, GICC, RETRO (model GlobFIRM used)	Y	1850	Lamarque et al. (2010)
CMIP6	Merged monthly fire carbon emis., present-day veg. dist., emis. factor	GFED4s, <a href="#">median of six</a> FireMIP model <a href="#">sims,s</a> , GCDv3 charcoal records, WMO visibility obs.	Y	1750	van Marle et al. (2017)

Acronym: GFED4: Global Fire Emissions Dataset version 4; GFED4s: GFED4 with small fires; GFAS1.2: Global Fire Assimilation System version 1.2; FINN1.5: Fire Inventory from NCAR version 1.5; FRP: fire radiative power; FEER1: Fire emissions from the Fire Energetics and Emissions Research version1; QFED2.5: Quick Fire Emissions Dataset version 2.5; AOD: aerosol optical depth; GFED2: GFED version 2; RETRO: REanalysis of the TROpospheric chemical composition; GICC: Global Inventory for Chemistry-Climate studies; GCDv3: Global Charcoal Database version

3

**Table 65.** Global total of fire emissions from 2003 to 2008 for DGVMs in FireMIPand benchmarks. Unit: Pg (Pg=10<sup>15</sup>g)

Source	C	CO <sub>2</sub>	CO	CH <sub>4</sub>	BC	OC	PM <sub>2.5</sub>
<b>FireMIP</b>							
CLM4.5	2.1	6.5	0.36	0.018	0.0021	0.020	0.042
CTEM	3.0	8.9	0.48	0.025	0.0028	0.030	0.060
JSBACH	2.1	6.5	0.32	0.013	0.0020	0.016	0.036
JULES	2.1	6.9	0.44	0.024	0.0022	0.020	0.039
LGG	4.9	15.4	0.90	0.047	0.0050	0.048	0.097
LGS	1.7	5.6	0.26	0.011	0.0017	0.012	0.027
LGSB	2.5	7.7	0.48	0.025	0.0025	0.024	0.047
MC2	1.0	3.1	0.18	0.008	0.0011	0.012	0.025
ORCHIDEE	2.8	9.2	0.44	0.018	0.0029	0.020	0.045
<b>Benchmarks</b>							
GFED4	1.5	5.4	0.24	0.011	0.0013	0.012	0.025
GFED4s	2.2	7.3	0.35	0.015	0.0019	0.016	0.036
GFAS1.2	2.1	7.0	0.36	0.019	0.0021	0.019	0.030
FINN1.5	2.0	7.0	0.36	0.017	0.0021	0.022	0.039
FEER1	4.2	14.0	0.65	0.032	0.0042	0.032	0.054
QFED2.5	----	8.2	0.39	0.017	0.0060	0.055	0.086

**Table 76.** Temporal correlation of annual global fire PM<sub>2.5</sub> emissions between FireMIP models and satellite-based GFED4 and GFED4s (1997–2012), GFAS1.2 and QFED2.5 (2001–2012), and FINN1.5 and FEER1 (2003–2012).

DGVMs	GFED4	GFED4s	GFAS1.2	FINN1.5	FEER1	QFED2.5
CLM4.5	0.73***	0.79***	0.63**	0.62*	0.55*	0.58**
CTEM	0.51**	0.54**	0.63**	0.60*	0.52	0.68**
JSBACH	-0.18	-0.42	0.10	0.02	-0.04	0.32
JULES	0.33	0.31	0.31	0.56*	0.29	0.39
LGG	0.08	0.03	-0.15	0.01	-0.20	-0.03
LGS	0.12	0.04	-0.00	0.40	-0.01	0.08
LGSB	0.51**	0.64***	0.39	0.72**	0.56*	0.55*
ORCHIDEE	-0.13	-0.25	-0.16	0.29	-0.10	-0.10

\*, \*\*, and \*\*\* : Pearson correlation passed the Student’s t-test at the 0.1, 0.05, and 0.01 significance level, respectively.

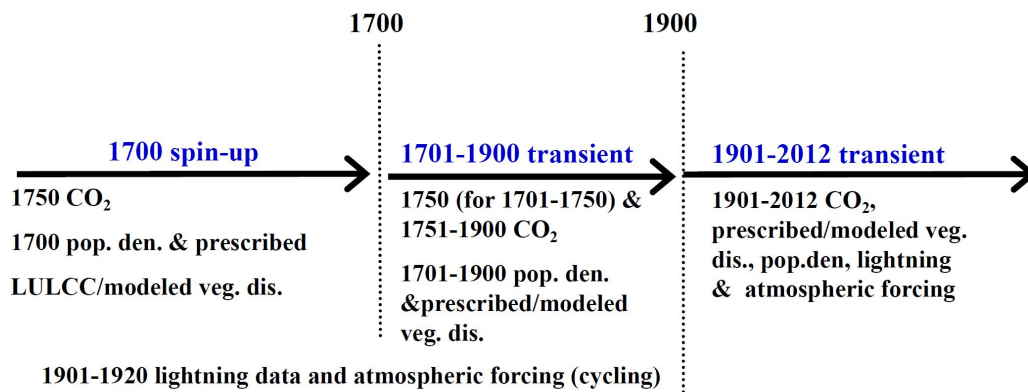


**Figure 1.** FireMIP experiment design. Note that CTEM and MC2 start at 1861 and 1901 and spin-up using 1861 and 1901 CO<sub>2</sub>, population density, and prescribed / modeled vegetation distribution, respectively.

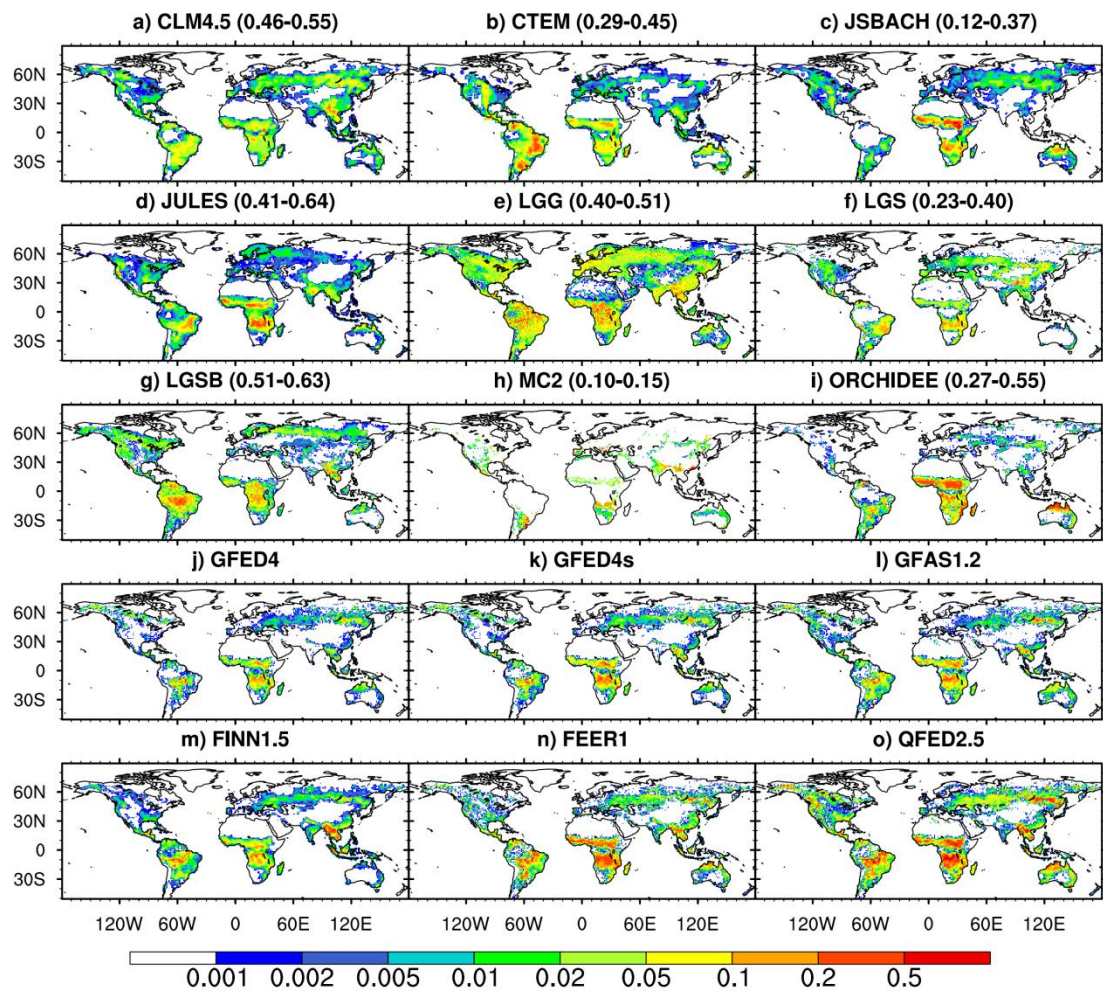


**Figure 2.** Spatial distribution of annual fire black carbon (BC) emissions ( $\text{g BC m}^{-2} \text{yr}^{-1}$ ) averaged over 2003–2008. The range of global spatial correlation between DGVMs and satellite-based products is also given in brackets.

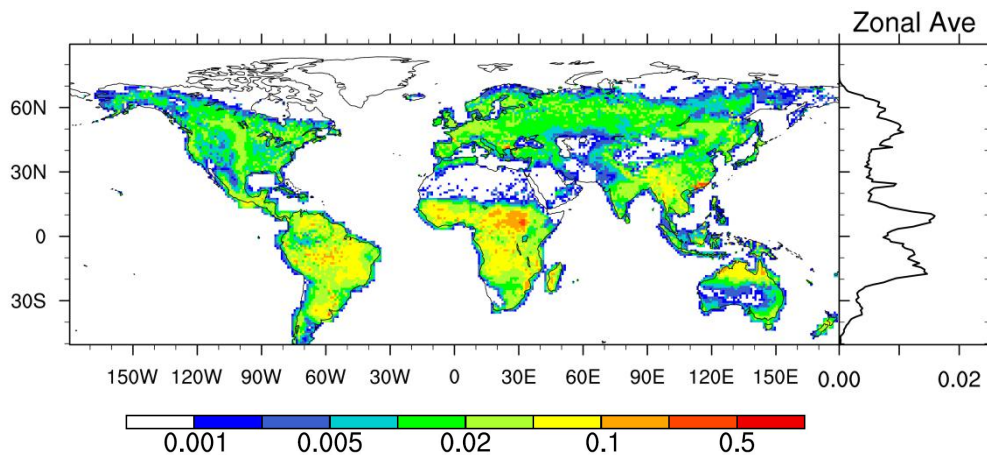


**Figure 3.** Inter-model standard deviation of 2003–2008 averaged fire BC emissions (g BC m<sup>-2</sup> yr<sup>-1</sup>) in FireMIP models and the zonal average.

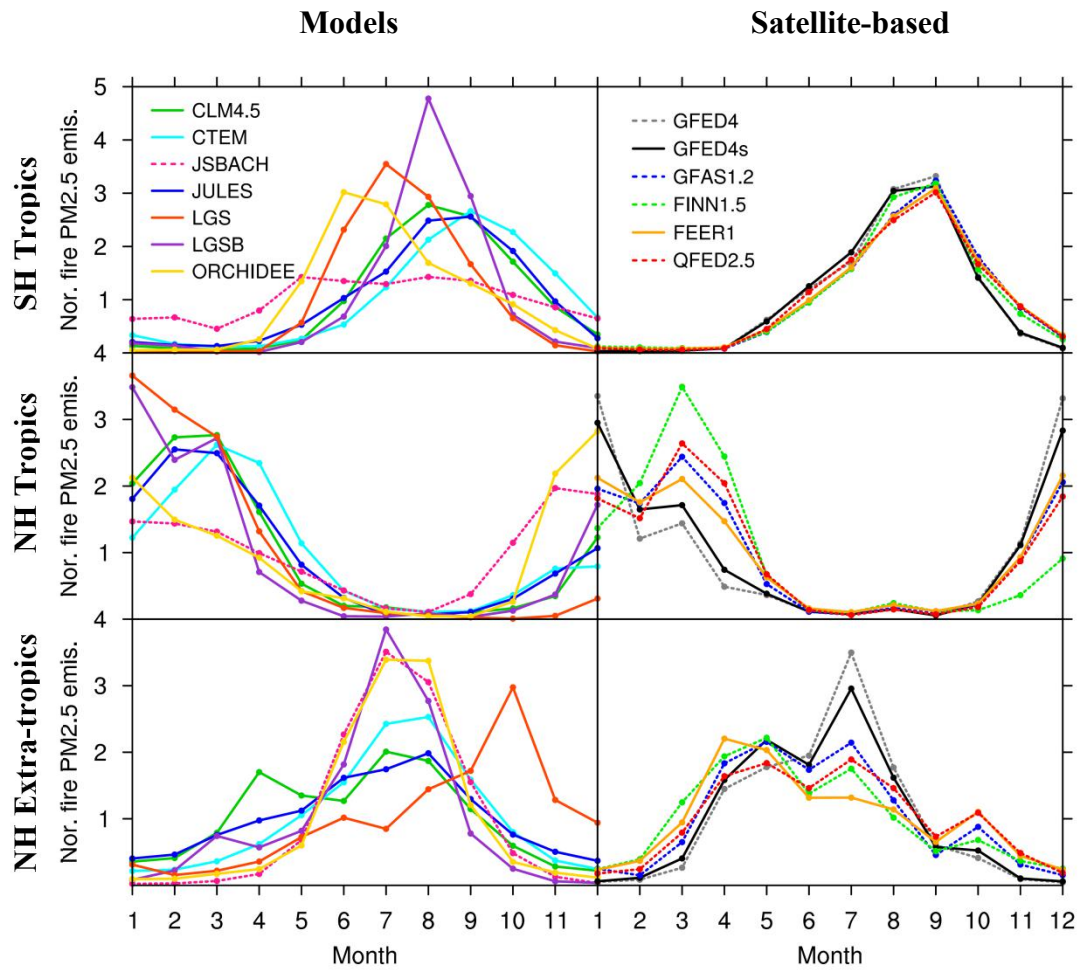


**Figure 4.** Seasonal cycle of fire  $PM_{2.5}$  emissions normalized by the mean from FireMIP models and satellite-based products averaged over 2003–2008 in the Southern Hemisphere (SH) tropics ( $0\text{--}23.5^{\circ}\text{S}$ ), Northern Hemisphere (NH) tropics ( $0\text{--}23.5^{\circ}\text{N}$ ), and NH extra-tropics ( $23.5\text{--}90^{\circ}\text{N}$ ). Fire emissions from LPJ-GUESS-GlobFIRM and MC2 are updated annually and thus are not included here.

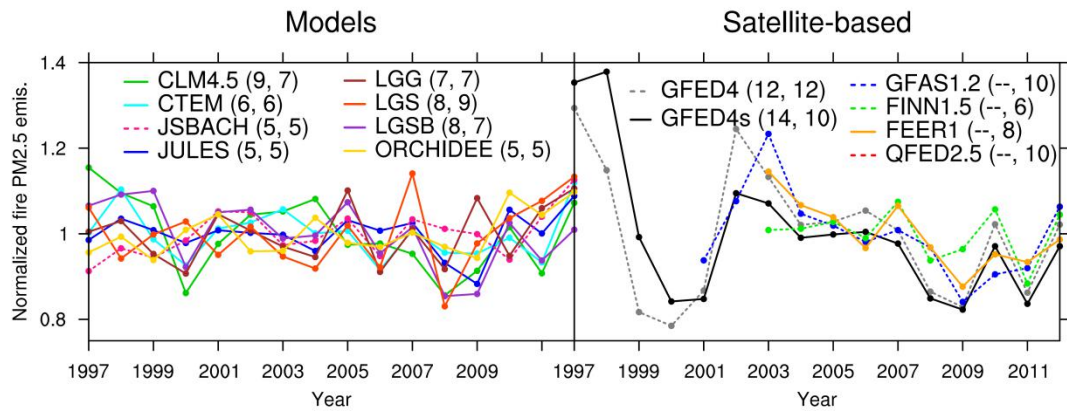


**Figure 5.** Temporal change of annual global fire  $PM_{2.5}$  emissions normalized by the mean from FireMIP models and satellite-based products. The numbers in the brackets are coefficient of variation (CV, the standard deviation divided by the mean, unit: %) for 1997–2012 and 2003–2012, respectively.

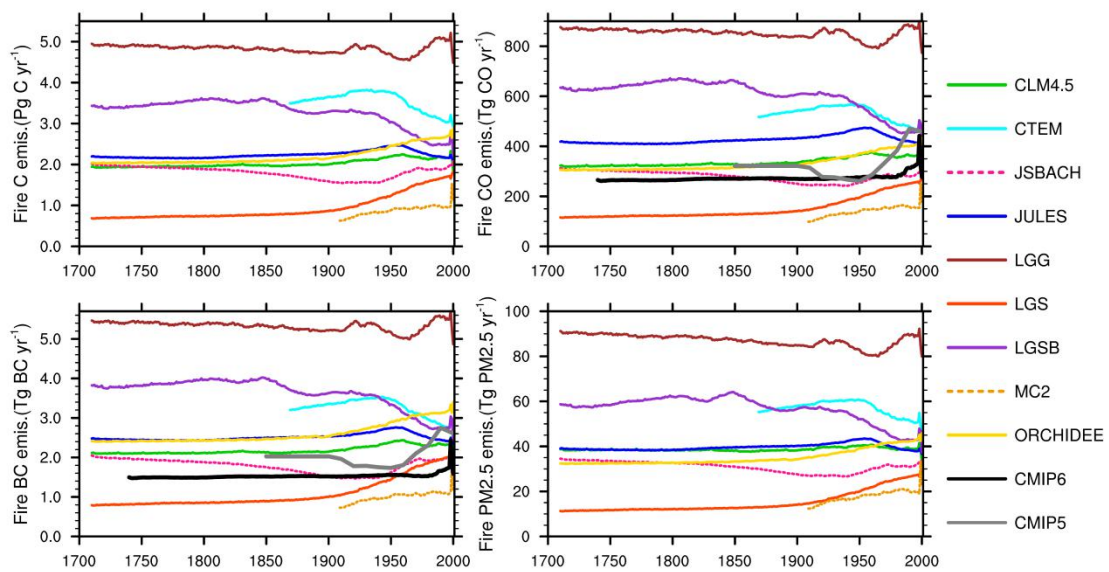


**Figure 6.** Long-term temporal change of fire emissions from DGVMs in FireMIP and CMIPs forcing. A 21-year running mean is used.

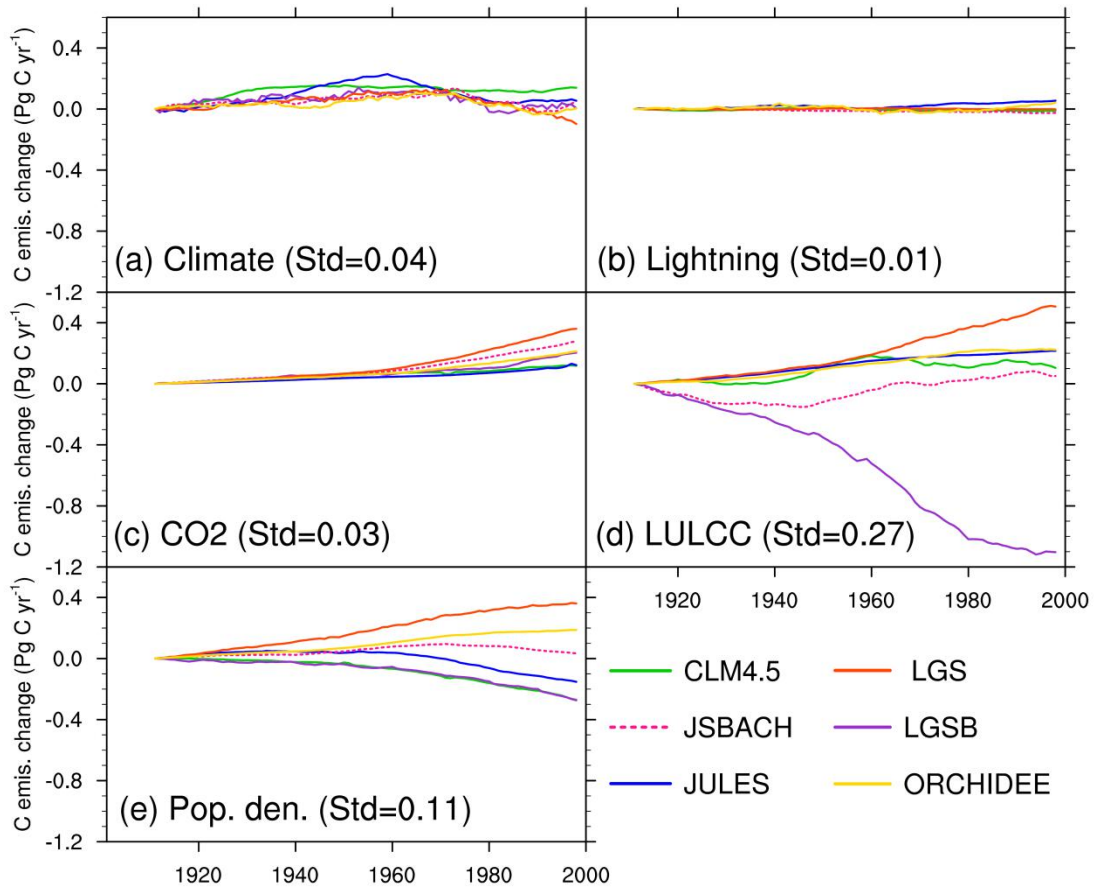


**Figure 7.** Change in global annual fire carbon emissions ( $\text{Pg C yr}^{-1}$ ) in the 20th century due to changes in (a) climate, (b) lightning frequency, (c) atmospheric  $\text{CO}_2$  concentration, (d) land use and land cover change (LULCC), and (e) population density (control run – sensitivity run). A 21-year running mean is used. The standard deviation (Std) of multi-model simulated long-term changes averaged over the 20th century is also given in the bracket. Control run is normal transient run, and five sensitivity runs are similar to the control run but without change in climate, lightning frequency, atmospheric  $\text{CO}_2$  concentration, land cover, and population density, respectively. The 20th century changes of driving forces used in FireMIP are characterized by an increase in the global land temperature, precipitation, lightning

frequency, atmospheric CO<sub>2</sub> concentration, and population density, expansion of croplands and pastures, and a decrease in the global forest area.

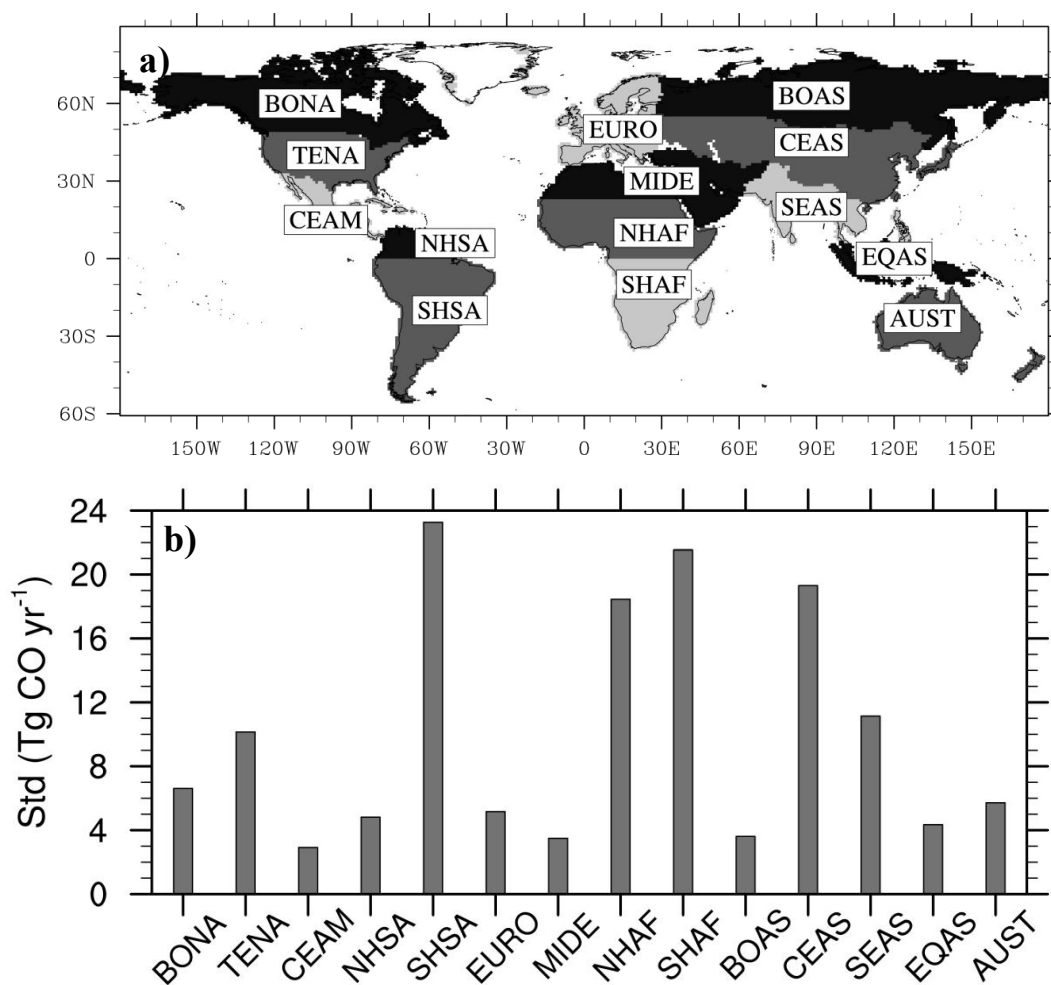


**Figure 8.** a) GFED region definition (<http://www.globalfiredata.org/data.html>), and b) inter-model discrepancy (quantified using inter-model standard deviation) in long-term changes (a 21-year running mean is used, relative to present-day) of simulated regional fire CO emissions (Tg CO yr<sup>-1</sup>) averaged over 1700–2012 (calculate long-term changes relative to present-day for each FireMIP model first, then the inter-model standard deviation, and lastly the time-average). Acronyms are

BONA: Boreal North America; TENA: Temperate North America; CEAM: Central America; NHSA: Northern Hem. South America; SHSA: Southern Hem. South America; EURO: Europe; MIDE: Middle East; NHAF: Northern Hem. Africa; SHAF: Southern Hem. Africa; BOAS: Boreal Asia; CEAS: Central Asia; SEAS: Southeast Asia; EQAS: Equatorial Asia; AUST: Australia.

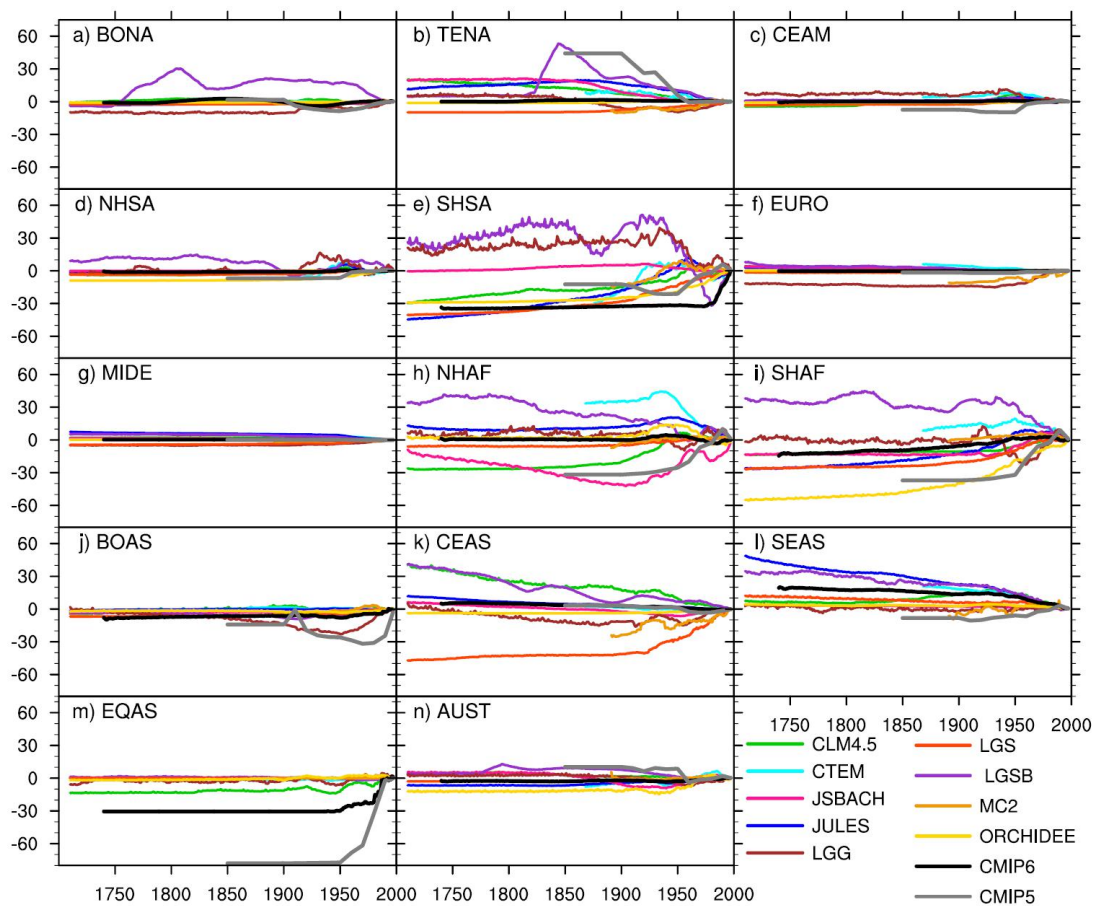


**Figure 9.** Long-term changes of annual regional fire CO emissions ( $\text{Tg CO yr}^{-1}$ ) from FireMIP models and CMIPs for regions with highest inter-model discrepancy in long-term changes of regional fire emissions shown in Fig. 8. A 21-year running mean is used.

